國 立 交 通 大 學

電信工程學系碩士班
碩士論文

於時間相關通道下之
雙模式有限回授傳送波束形成技術

Transmit Beamforming with Dual-Mode Limited

Feedback over Temporally-Correlated Channels

研 究 生：陳亮元　　　　　Student: Liang-Yuan Chen

指導教授：李大嵩 博士　　　Advisor: Dr. Ta-Sung Lee

中 華 民 國 九 十 六 年 六 月

於時間相關通道下之

雙模式有限回授傳送波束形成技術

Transmit Beamforming with Dual-Mode Limited

Feedback over Temporally-Correlated Channels

研 究 生：陳亮元　　　　　Student: Liang-Yuan Chen

指導教授：李大嵩 博士　　　Advisor: Dr. Ta-Sung Lee

國立交通大學

電信工程學系碩士班

碩士論文

A Thesis
Submitted to Institute of Communication Engineering
College of Electrical and Computer Engineering
National Chiao Tung University
in Partial Fulfillment of the Requirements
for the Degree of
Master of Science
in
Communication Engineering
June 2007
Hsinchu, Taiwan, Republic of China

中 華 民 國 九 十 六 年 六 月

於時間相關通道下之
雙模式有限回授傳送波束形成技術

學生：陳亮元　　　　　　　　指導教授：李大嵩 博士

國立交通大學電信工程學系碩士班

摘要

在新一代無線通訊中，有限回授前置編碼（Limited Feedback Precoding）為一用以提升系統可靠度的技術，其特色在由接收機回傳最佳前置編碼的編號給發射機，且發射機不需要任何的通道狀態資訊。在本論文中，吾人主要探討在多輸入單輸出（Multiple-Input Single-Output, MISO）系統中的傳送波束形成技術（Transmit Beamforming）；傳統的作法，在固定平均回授率的情況下，單一模式有限回授系統（只有一個編碼簿）在時變通道下並不夠強健。假設接收端有完整的通道狀態資訊、無錯誤的回授通道，和一階馬可夫多輸入單輸出通道模型，吾人提出一個雙模式有限回授系統和基於符元錯誤率的模式選擇準則，在連續的兩個單位時間內，考慮兩種傳送波束形成模式：（1）在每個獨立的單位時間內，用較小容量的編碼簿個別作波束形成；（2）在兩個單位時間內，用較大容量的編碼簿聯合作波束形成。利用連續兩個單位時間內的時間相關係數和完整的通道狀態資訊，吾人提出的模式選擇準則，可以選擇較佳的模式傳輸。由模擬結果可以看出雙模式有限回授前置編碼系統效能優於單模式有限回授前置編碼系統。

Transmit Beamforming with Dual-Mode Limited Feedback over Temporally-Correlated Channels

Student: Liang-Yuan Chen   Advisor: Dr. Ta-Sung Lee

Department of Communication Engineering

National Chiao Tung University

Abstract

Limited feedback precoding is a technique used to improve system reliability in modern wireless communications. The feature of limited feedback precoding is that receiver feeds back the index of the optimal precoder to the transmitter. The transmitter does not need to have any channel state information (CSI). In this thesis, we focus on the transmit beamforming scheme in multiple-input single-output (MISO) systems. In conventional approach, under a fixed average feedback rate, the single-mode limited feedback system (has only one codebook) is not robust enough in time-varying channels. Perfect channel knowledge known at the receiver, error-free feedback channel, and first-order Markov MISO channel model are assumed in this thesis. We propose a dual-mode limited feedback system with a symbol-error-rate (SER) based mode selection criterion. Two transmit beamforming modes over two consecutive time slots are considered: (1) separate beamforming for the individual time slot with a small-size codebook, and (2) joint beamforming for both slots with a large-size codebook. By exploiting the temporal-correlation coefficient of two consecutive time slots and perfect channel knowledge, the better mode can be selected by using the mode selection criterion. Simulation results show that the performance of the dual-mode limited feedback system is better than that of the single-mode limited feedback system.

Acknowledgement

I would like to express my deepest gratitude to my advisor, Dr. Ta-Sung Lee, for his enthusiastic guidance and great patience. I learn a lot from his positive attitude in many areas. Heartfelt thanks are also offered to all members in the Communication System Design and Signal Processing (CSDSP) Lab for their constant encouragement. Finally, I would like to show my sincere thanks to my parents for their invaluable love.

Contents

List of Figures

List of Tables

Acronym Glossary

AWGN   additive white Gaussian noise

BER   bit error rate

CDF   cumulative distribution function

CP   cyclic prefix

CSI   channel state information

DFT   discrete Fourier transform

IEEE   institute of electrical and electronics engineers

FFT   fast Fourier transform

MIMO   multiple-input multiple-output

MISO   multiple-input single-output

MSE   mean square error

MMSE   minimum mean square error

OFDM   orthogonal frequency division multiplexing

PDF   probability density function

QAM   quadrature amplitude modulation

SER   symbol error rate

SNR   signal-to-noise ratio

SVD   singular value decomposition

ZF   zero forcing
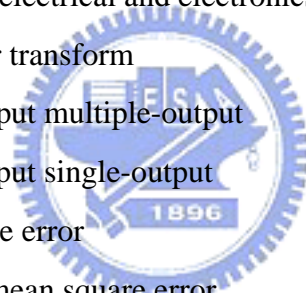
Notations

b	number of bits required for the index that indicate any codeword in the codebook
$\mathbf{A}_{j,k}$	entry (j,k) of matrix $\mathbf{A}$
E_s	symbol energy
$\mathbf{E}\{\cdot\}$	expected value
$\mathcal{F}$	precoder or beamformer set
$\mathbf{f}_k$	beamformer for the k th frame or time slot
$\mathbf{F}_k$	precoding matrix for the k th frame or time slot
$\mathbf{H}_k$	MIMO channel matrix for the k th frame or time slot
h_i^k	channel gain between the i th transmit and receive antenna for the k th frame or time slot in MISO system
L	frame length
L_{ch}	channel order
M	number of substreams
N_{FFT}	FFT length
N_{CP}	CP length
N_t	number of transmit antennas
N_r	number of receive antennas
N_0	noise power spectrum density
P_M	symbol error rate of M-QAM constellation
$\mathbf{n}_k$	noise vector for the k th frame or time slot
$\mathbf{V}_L$	left singular matrix of channel matrix $\mathbf{H}$
$\mathbf{V}_R$	right singular matrix of channel matrix $\mathbf{H}$
$\boldsymbol{\Lambda}$	singular value matrix of channel matrix $\mathbf{H}$
$\bar{\mathbf{V}}_R$	matrix formed from the first M columns of $\mathbf{V}_R$

$y_{k,i}$	received signal at the ith receive antenna for the kth frame or time slot
k	frame index or time slot index
$z_{k,i}$	transmitted signal from the ith transmit antenna for the kth frame or time slot
$n_{k,i}$	additive white noise at the ith receive antenna for the kth frame or time slot
σ_n^2	noise power
ρ	temporal-correlation coefficient
γ	signal-to-noise ratio
$(\cdot)^+$	matrix pseudo-inverse
$\gamma_{k,\mathrm{mode1}}$	average SNR over the kth frame or time slot in Mode I
$\gamma_{k,\mathrm{mode2}}$	average SNR over the kth frame or time slot in Mode II
$SER_{k,\mathrm{mode1}}$	average SER over the kth frame or time slot in Mode I
$SER_{k,\mathrm{mode2}}$	average SER over the kth frame or time slot in Mode II
$\overline{SER}_{\mathrm{mode1}}$	average SER over consecutive frames or time slots in Mode I
$\overline{SER}_{\mathrm{mode2}}$	average SER over consecutive frames or time slots in Mode II
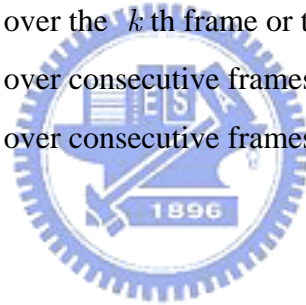
Chapter 1

Introduction

Wireless systems employing multiple antenna arrays at both the transmitter and receiver, known as multiple-input multiple output (MIMO) systems, promise high capacity and high-quality wireless communication links [1]. MIMO systems improve quality, capacity, and reliability. Two popular approaches for communicating in the MIMO channel are diversity and spatial multiplexing.

MIMO diversity is an approach in which information is spread across multiple transmit antennas to maximize the diversity gain in the MIMO channel. One of the popular schemes for space-time diversity coding is Alamouti scheme [2]. It provides full transmit diversity and full code rate for MIMO systems with two transmit antennas.

When channel state information (CSI) is known at the transmitter, diversity can be obtained using space-time codes (STC) [2]-[3] and transmit precoding. Transmit precoding which exploits the channel state information at the transmitter can increase various performance gains for wireless communication [4]. The design of the precoders based on different forms of the channel information available to the transmitter recently draws much attention [5]-[8]. With exact feedback of the channel state information, optimal precoders in terms of maximal channel capacity, minimal bit-error-rate (BER), and minimal symbol mean square errors were reported in [9] and [10]. Another simple

approaches used to improve the system performance are transmit beamforming and receive combining. Compared with space-time codes, transmit beamforming and receive combining achieve the same diversity order as well as additional array gain. It can significantly improve the system performance [11]-[13].

CSI known at the transmitter is not a practical assumption. Furthermore, conveying full CSI through a feedback channel is also impractical because the channel coefficients need to be quantized and fed back to the transmitter over limited bandwidth channels. Thus, limited feedback precoding schemes are proposed to solve the problem.

In limited feedback precoded systems, receivers use current CSI to select the optimal precoder from a given codebook and feed back the codeword index through the limited bandwidth control channel [14]-[19]. Most of the existing works on the limited feedback precoidng focus on the development of quantization criteria and the related performance analysis. Limited feedback precoding was also mentioned in the technical reports of IEEE 802.16-2005 standard [20]-[23]. Another important issue is the optimal codebook design. Optimal codebook design is a problem of Grassmannian line packing [24]. The problem has been solved and the optimal codebooks with different dimensions and sizes are also constructed in [24]. The optimal codebooks are also considered in IEEE 802.16-2005 standard [25].

The single-mode limited feedback precoded system is a system that has only one codebook. Under a fixed average feedback rate, the single-mode limited feedback precoded system is not robust enough in mobile environments. Thus, the tradeoff problem is, "less feedback more often, or more feedback less often?"

In this thesis we study transmit beamforming with limited feedback when the channels between consecutive time slots are subject to temporal correlation. We assume that (1) two beamformer sets $\mathcal{F}_1$ and $\mathcal{F}_2$ (with, respectively, 2^b and 2^{2b} codewords)

are available, and (2) the average feedback rate is fixed in a transmission. We address the problem of beamforming strategy selection for two consecutive time slots. More specifically, relying on an average symbol-error-rate (SER) based criterion we wish to determine which one of the following two scheme is better: (i) separate beamforming for the individual time slot with $\mathcal{F}_1$, (ii) joint beamforming for both slots by using $\mathcal{F}_2$. The considered problem is motivated by the necessity of mode switching when the channels are time-varying, a scenario typically found in the mobile environment. We develop an SER based mode selection criterion for the temporal-correlation channel environment. Simulation results illustrate the advantage of the proposed method against those without mode selection.

This thesis is organized as follows. In Chapter 2, the overview of the limited feedback system and the precoder selection criteria are introduced. Moreover, MIMO precoding scheme in IEEE 802.16-2005 is also presented. In Chapter 3, single-mode limited feedback precoded system is introduced. We consider first-order Markov MISO channel model and use the codebooks defined for transmit beamforming in 802.16-2005 standard. SER performances of the single-mode limited feedback MISO system and MISO-OFDM (orthogonal frequency division multiplexing) system are also illustrated in this chapter under a fixed average feedback rate. In Chapter 4, the proposed dual-mode limited feedback systems and the SER based mode selection criterion for the temporal-correlation channel environment are presented and derived. Numerical experiments illustrate the advantage of the proposed method against those without mode selection. Finally, we conclude this thesis in Chapter 5.

Chapter 2

Limited Feedback Precoding for MIMO Systems

Digital communication using multiple-input multiple-output (MIMO) has recently emerged as one of the most significant technical breakthroughs in wireless communications. This technology figures on the list of recent technical advances with a chance of resolving the bottleneck of traffic capacity in future wireless communications. MIMO systems can provide high channel capacity and high reliability. When channel state information (CSI) is known at the transmitter, precoding can provide diversity gain and additional array gain. But the transmitter always has no knowledge about current CSI. In limited feedback precoded systems, the receiver selects the optimal precoder from a given codebook based on current CSI and feeds back the index of the optimal precoder to the transmitter [14]-[19].

This chapter focuses on the limited feedback techniques and precoder selection criteria. An overview of the limited feedback system will be given first. Then we introduce the precoder selection criteria used to select the optimal precoder from a given codebook. Finally, the limited feedback MIMO precoding scheme in IEEE 802.16-2005 standard is also introduced here.

2.1 Limited Feedback Systems

In MIMO wireless communications, precoding is often used to improve channel capacity and reliability. Many MIMO wireless systems, however, do not have current CSI at the transmitter because the forward and reverse channels lack reciprocity. The basic idea of limited feedback systems is to select the optimal precoder from a given codebook at the receiver rather than at the transmitter based on current CSI. Then the receiver feeds back the index of the optimal precoder to the transmitter. Precoder selection criteria used to select the optimal precoder are discussed in [14]-[19] and the optimal codebook design, which is a problem of Grassmannian line packing, is solved in [24].

In the following section, the limited feedback precoding MIMO channel model will be introduced. Then the decoding scheme of the limited feedback system for ZF and MMSE receivers will be presented in 2.1.2.
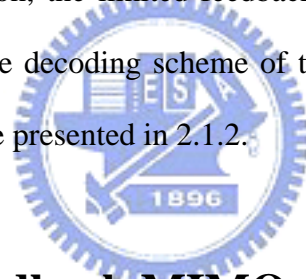
2.1.1 Limited Feedback MIMO Channel Model

The limited feedback MIMO system is illustrated in **Figure 2.1**. The MIMO system has N_t transmit antennas and N_r receive antennas. The receiver selects the optimal precoder based on current CSI and feeds back the index of the optimal precoder to the transmitter. M different substreams are precoded with the optimal precoder $\mathbf{F}_k$. Each of the M substreams is modulated independently using the same constellation $\mathcal{W}$. This yields a data symbol vector at time slot k of $\mathbf{s}_k = \left[s_{k,1}, s_{k,2}, ..., s_{k,M} \right]^T$. $s_{k,j}$ is the data symbol of the j th substream at time slot k and $\mathbf{E}_{\mathbf{s}_k} \left[\mathbf{s}_k \mathbf{s}_k^H \right] = E_s \cdot \mathbf{I}_M$. We assume that $\mathbf{E}_{\mathbf{s}_k} \left[\mathbf{s}_k \mathbf{s}_k^H \right] = E_s \cdot \mathbf{I}_M = \mathbf{I}_M$ for convenience.
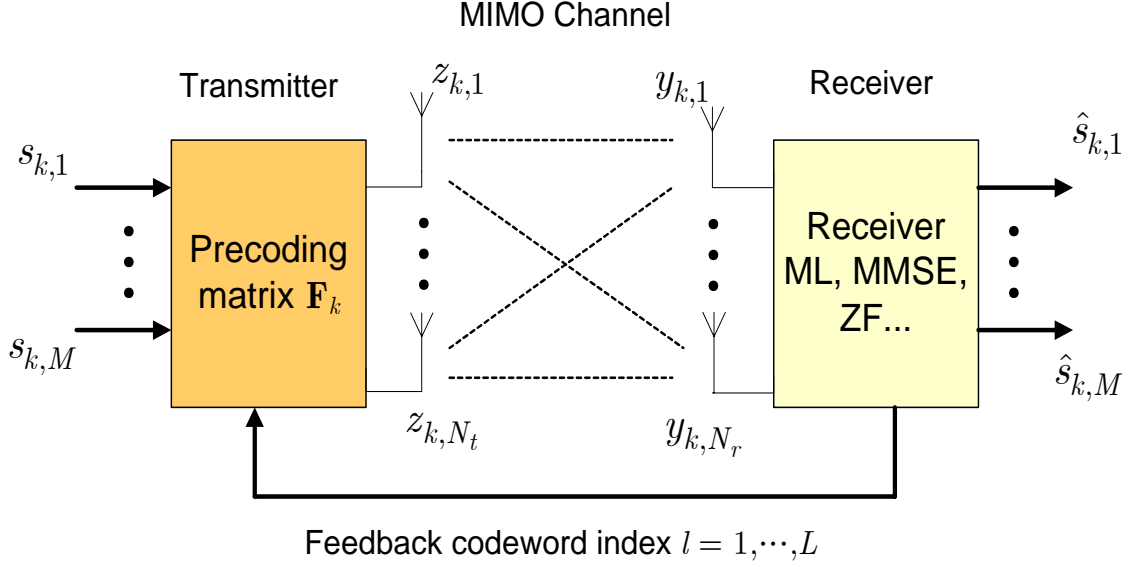
Figure 2.1: Limited feedback MIMO system architecture

The data symbol vector $\mathbf{s}_k$ is multiplied by an $N_t \times M$ precoder $\mathbf{F}_k$ which is selected as a function of the current CSI by using the precoder selection criteria. The transmit signal vector $\mathbf{z}_k = \left[z_{k,1}, \ldots, z_{k,N_t} \right]^T$ at time slot k can be written as

$$\mathbf{z}_k = \sqrt{\frac{E_s}{M}} \mathbf{F}_k \mathbf{s}_k, \tag{2.1}$$

where E_s is the symbol energy. Assuming perfect timing, synchronization, and sampling, the discrete-time equivalent received signal vector can be written as

$$\mathbf{y}_k = \sqrt{\frac{E_s}{M}} \mathbf{H}_k \mathbf{F}_k \mathbf{s}_k + \mathbf{n}_k, \tag{2.2}$$

where $\mathbf{H}_k$ is the $N_r \times N_t$ channel matrix and $\mathbf{n}_k$ is the $N_r \times 1$ noise vector at time slot k. The entries of $\mathbf{H}_k$ are independent and identically distributed (i.i.d.) according to $\mathcal{CN}(0,1)$ and the entries of $\mathbf{n}_k$ are independent and distributed according to $\mathcal{CN}(0,\sigma_n^2)$. The received signal vector is decoded by a vector decoder with perfect knowledge of $\mathbf{H}_k \mathbf{F}_k$ that produces a hard decoded symbol vector $\hat{\mathbf{s}}_k$.

The receiver selects a precoder $\mathbf{F}_k$ from a finite set of precoding matrices

$\mathcal{F} = \{\mathbf{F}_1, \mathbf{F}_2, ..., \mathbf{F}_N\}$ and feeds back the index of the selected precoder to the transmitter over a limited bandwidth, zero-delay feedback link. Each $\mathbf{F}_k \in \mathcal{F}$ is assumed to have orthogonal unit column vectors since it follows the form of the optimal, full channel knowledge precoders derived in [9] assuming a maximum singular value constraint of $\mathbf{F}_k$. The proposed codebook satisfies $\mathcal{F} \subset \mathcal{U}(N_t, M)$.

We assume that b bits of feedback are available. Thus, the codebook consists of $N = 2^b$ matrices in $\mathcal{U}(N_t, M)$. In this constraint, codebook design can be converted to a problem of Grassmannian line packing [24]. The limitation of the codebook to 2^b matrices allows the designer to constrain the precoding overhead and take full advantage of the limited feedback channel.

2.1.2 Decoding Scheme of Limited Feedback MIMO Systems
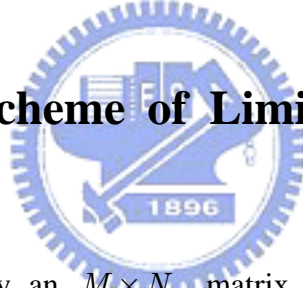
Linear receivers apply an $M \times N_r$ matrix $\mathbf{G}$ to produce the hard decoded symbol vector $\hat{\mathbf{s}}_k$, where $\hat{\mathbf{s}}_k = \mathbf{G}\mathbf{y}_k$. Criteria will be presented for two different forms of $\mathbf{G}$: zero-forcing (ZF) and minimum mean-square error (MMSE).

Zero-Forcing (ZF) Receiver

For a zero-forcing linear receiver, the decoding matrix $\mathbf{G}$ is defined as

$$\mathbf{G} = (\mathbf{H}_k \mathbf{F}_k)^+, \tag{2.3}$$

where $(\cdot)^+$ is the matrix pseudo-inverse, $\mathbf{H}_k$ is the channel matrix, and $\mathbf{F}_k$ is the precoding matrix. Perfect CSI known at the receiver is assumed. The hard decoded symbol vector $\hat{\mathbf{s}}_k$ from the ZF decoder can be written as

$$\hat{\mathbf{s}}_k = \mathbf{G}\mathbf{y}_k = \sqrt{\frac{E_s}{M}} \left(\mathbf{H}_k \mathbf{F}_k\right)^+ \mathbf{H}_k \mathbf{F}_k \mathbf{s}_k + \left(\mathbf{H}_k \mathbf{F}_k\right)^+ \mathbf{n}_k$$

$$= \underbrace{\sqrt{\frac{E_s}{M}}\left(\mathbf{I}_M\right)\mathbf{s}_k}_{\text{signal}} + \underbrace{\left(\mathbf{H}_k \mathbf{F}_k\right)^+ \mathbf{n}_k}_{\text{noise}}. \tag{2.4}$$

Minimum Mean-Square Error (MMSE) Receiver

For an MMSE linear receiver, the decoding matrix $\mathbf{G}$ is defined as

$$\mathbf{G} = \left(\mathbf{F}_k^H \mathbf{H}_k^H \mathbf{H}_k \mathbf{F}_k + \frac{MN_0}{E_s}\mathbf{I}_M\right)^{-1} \mathbf{F}_k^H \mathbf{H}_k^H, \tag{2.5}$$

where M is the number of substreams, N_0 is the noise power spectrum density, and E_s is the symbol energy. The hard decoded symbol vector $\hat{\mathbf{s}}_k$ of the MMSE decoder can be written as

$$\hat{\mathbf{s}}_k = \mathbf{G}\mathbf{y}_k$$

$$= \sqrt{\frac{E_s}{M}}\left(\mathbf{F}_k^H \mathbf{H}_k^H \mathbf{H}_k \mathbf{F}_k + \frac{MN_0}{E_s}\mathbf{I}_M\right)^{-1} \mathbf{F}_k^H \mathbf{H}_k^H \mathbf{H}_k \mathbf{F}_k \mathbf{s}_k$$

$$+ \left(\mathbf{F}_k^H \mathbf{H}_k^H \mathbf{H}_k \mathbf{F}_k + \frac{MN_0}{E_s}\mathbf{I}_M\right)^{-1} \mathbf{F}_k^H \mathbf{H}_k^H \mathbf{n}_k$$

$$= \underbrace{\sqrt{\frac{E_s}{M}}\left(\mathbf{F}_k^H \mathbf{H}_k^H \mathbf{H}_k \mathbf{F}_k + \frac{MN_0}{E_s}\mathbf{I}_M\right)^{-1}\left(\mathbf{I}_M\right)\mathbf{s}_k}_{\text{signal}} + \underbrace{\left(\mathbf{F}_k^H \mathbf{H}_k^H \mathbf{H}_k \mathbf{F}_k + \frac{MN_0}{E_s}\mathbf{I}_M\right)^{-1} \mathbf{F}_k^H \mathbf{H}_k^H \mathbf{n}_k}_{\text{noise}}.$$

$$\tag{2.6}$$

The MMSE receiver is more complex than the ZF receiver. However, it has better performance in noise reduction and reliability.

2.2 Precoder Selection Criteria

In this section, we will introduce the precoder selection criteria proposed in [16] used for selecting the optimal percoder from a given codebook. Three precoder selection criteria will be introduced here: (1) capacity selection criterion (Capacity-SC), (2) MSE selection criterion (MSE-SC), and (3) minimum singular value selection criterion (MSV-SC).

2.2.1 Capacity Selection Criterion

When the transmitter is precoded with the precoder $\mathbf{F}$, the equivalent channel is $\mathbf{HF}$. The mutual information assuming an uncorrelated complex Gaussian source given $\mathbf{H}$ and a fixed $\mathbf{F}$ is

$$I\left(\mathbf{F}\right) = \log_2 \det\left(\mathbf{I}_M + \frac{E_s}{MN_0}\mathbf{F}^H\mathbf{H}^H\mathbf{HF}\right). \tag{2.7}$$

The capacity selection criterion is stated as follows:

Capacity Selection Criterion (Capacity-SC):

Pick $\mathbf{F}$ such that

$$\mathbf{F} = \arg\max_{\mathbf{F}_i \in \mathcal{F}} I\left(\mathbf{F}_i\right), \tag{2.8}$$

where $\mathcal{F}$ is the precoder set. Capacity selection criterion can improve the effective channel capacity and the optimal unquantized precoder is $\mathbf{F}_{\text{opt}} = \overline{\mathbf{V}}_R$, which is proved in [16]. $\overline{\mathbf{V}}_R$ is the matrix formed from the first M columns of $\mathbf{V}_R$ and $\mathbf{V}_R$ is the right singular matrix of the channel matrix $\mathbf{H}$.

2.2.2 Mean Square Error Selection Criterion

For a linear MMSE receiver, the precoder is selected to either minimize the trace of the mean square error matrix or minimize the determinant of the mean square error matrix. The linear MMSE decoder is defined as

$$\mathbf{G} = \left(\mathbf{F}^H \mathbf{H}^H \mathbf{H} \mathbf{F} + \frac{MN_0}{E_s} \mathbf{I}_M \right)^{-1} \mathbf{F}^H \mathbf{H}^H. \tag{2.9}$$

The MSE can be expressed as

$$\overline{\mathrm{MSE}}(\mathbf{F}) = \frac{E_s}{M} \left(\mathbf{I}_M + \frac{E_s}{MN_0} \mathbf{F}^H \mathbf{H}^H \mathbf{H} \mathbf{F} \right)^{-1}. \tag{2.10}$$

Using (2.10), the MSE selection criterion is stated as follows:

Mean Square Error Selection Criterion (MSE-SC):

Pick **F** such that

$$\mathbf{F} = \arg \min_{\mathbf{F}_i \in \mathcal{F}} m\big(\overline{\mathrm{MSE}}(\mathbf{F}_i) \big), \tag{2.11}$$

where $m(\cdot)$ denotes either $\det(\cdot)$ or $\mathrm{trace}(\cdot)$. MSE selection criterion can improve the overall system performance and the optimal unquantized precoder is $\mathbf{F}_{\mathrm{opt}} = \bar{\mathbf{V}}_R$ which is also proved in [16].

2.2.3 Minimum Singular Value Selection Criterion

For a linear ZF receiver, the precoder is selected to minimize the bound on the average probability of a symbol vector error. The linear ZF decoder is defined as

$$\mathbf{G} = (\mathbf{H} \mathbf{F})^+, \tag{2.12}$$

where $(\cdot)^+$ is the matrix pseudo-inverse. From [17], the SNR of the k th substream is given by

$$\text{SNR}_k^{(\text{ZF})} = \frac{E_s}{MN_0 \left[\mathbf{F}^H \mathbf{H}^H \mathbf{H} \mathbf{F} \right]_{k,k}^{-1}}, \tag{2.13}$$

where $\mathbf{A}_{k,k}^{-1}$ is entry (k,k) of $\mathbf{A}^{-1}$.

The work in [17] shows that in order to minimize a bound on the average probability of a symbol vector error, the minimum substream SNR must be maximized. Using a selection criterion based on the minimum SNR requires the computation of the SNR of all substreams. The high computational complexity results in hard implementation. For the reason, [17] shows that the minimum SNR for ZF can be bounded by

$$\text{SNR}_{\min}^{(\text{ZF})} = \min_{1 \le k \le M} \text{SNR}_k^{(\text{ZF})} \ge \lambda_{\min}^2 \{\mathbf{HF}\} \frac{E_s}{MN_0}, \tag{2.14}$$

where $\lambda_{\min}\{\mathbf{HF}\}$ is the minimum singular value of $\mathbf{HF}$. Using (2.14), the minimum singular value selection criterion is stated as follows:

Minimum Singular Value Selection Criterion (MSV-SC):

Pick $\mathbf{F}$ such that

$$\mathbf{F} = \arg \max_{\mathbf{F}_i \in \mathcal{F}} \lambda_{\min} \{\mathbf{HF}_i\}. \tag{2.15}$$

From [17], the minimum singular value selection criterion provides a close approximation to maximizing the minimum SNR for ZF receiver and the optimal unquantized precoder is $\mathbf{F}_{\text{opt}} = \overline{\mathbf{V}}_R$ which is also proved in [16].

2.3 Codebooks for MIMO Precoding Scheme in IEEE 802.16-2005

Codebooks with different dimensions and sizes are defined in IEEE 802.16-2005 standard [25]. All codebooks are divided into two kinds: 3-bit codebooks and 6-bit codebooks. The codebooks for 2x1, 3x1, and 4x1 with 3-bit feedback index are listed in **Table 2.1**, **Table 2.2**, and **Table 2.3**. The notation $V(N_t, S, L)$ denotes the vector codebook, which consists of 2^L complex, unit vectors of a dimension N_t. S denotes the number of substreams. The interger L is the number of bits required for the index that can indicate any matrix in the codebook.

Table 2.1: MIMO precoding codebook $V(2,1,3)$

Vector index	1	2	3	4	5	6	7	8
v1	1	0.7490	0.7490	0.7491	0.7491	0.3289	0.0.5112	0.3289
v2	0	-0.5801 +j0.1818	0.0576 +j0.6051	-0.2978 -j0.5298	-0.6038 +j0.0689	-0.6614 +j0.6740	-0.4754 -j0.7160	-0.8779 -j0.3481

Table 2.2: MIMO precoding codebook $V(3,1,3)$

Vector index	1	2	3	4	5	6	7	8
v1	1	0.5	0.5	0.5	0.5	0.4954	0.5	0.5
v2	0	-0.7201 -0.3126i	-0.0659 +0.1371i	-0.0063 +0.6527i	0.7171 +0.3202i	0.4819 -0.4517i	0.0686 -0.1386i	-0.0054 -0.654i
v3	0	0.2483 -0.2684i	-0.6283 -0.5763i	0.4621 -0.3321i	-0.2533 +0.2626i	0.2963 -0.4801i	0.6200 +0.5845i	-0.4566 +0.3374i

Table 2.3: MIMO precoding codebook $V(4,1,3)$

Vector index	1	2	3	4	5	6	7	8
v1	1	0.3780	0.3780	0.3780	0.3780	0.3780	0.3780	0.3780
v2	0	-0.2698 -0.5668i	-0.7103 +0.1326i	0.2830 -0.094i	-0.0841 +0.6478i	0.5247 +0.3532i	0.2058 -0.1369i	0.0618 -0.3332i
v3	0	0.5957 +0.1578i	-0.235 -0.1467i	0.0702 -0.8261i	0.0184 +0.049i	0.4115 +0.1825i	-0.5211 +0.0833i	-0.3456 +0.5029i
v3	0	0.1587 -0.2411i	0.1371 +0.4893i	-0.2801 +0.0491i	-0.3272 -0.5662i	0.2639 +0.4299i	0.6136 -0.3755i	-0.5704 +0.2133i

In IEEE 802.16-2005 standard [25], three operations are employed and they employ floating point arithmetic in IEEE Standard 754, whose final results are rounded to four decimal places. The first operation is introduced as follows and generates an unitary $N \times N$ matrix $H(\mathbf{v})$ using an $N \times 1$ vector $\mathbf{v}$ as

$$H(\mathbf{v}) = \begin{cases} \mathbf{I}, & \mathbf{v} = \mathbf{e}_1 \\ I - p\mathbf{w}\mathbf{w}^H, & \text{otherwise} \end{cases}, \tag{2.16}$$

where $\mathbf{w} = \mathbf{v} - \mathbf{e}_1$, $\mathbf{e}_1 = [1,0,...,0]^T$, $p = \dfrac{2}{\left\| \mathbf{w}^H \mathbf{w} \right\|^2}$, and $\mathbf{I}$ is the identity matrix.

The second operation generates an $N \times (M+1)$ unitary matrix from a unit $N \times 1$ vector and a unitary $(N-1) \times M$ matrix as

$$HC\left(\mathbf{v}_N, \mathbf{A}_{(N-1) \times M}\right) = H\left(\mathbf{v}_N\right) \begin{bmatrix} 1 & 0 & \cdots & & 0 \\ 0 & & & & \\ \vdots & & & & \\ 0 & & & \mathbf{A}_{(N-1) \times M} \end{bmatrix}, \tag{2.17}$$

where $N - 1 \geq M$ and the $(N-1) \times M$ unitary matrix has property $\mathbf{A}^H \mathbf{A} = \mathbf{I}$. The third operation generates an $N \times M$ matrix from a unit $N \times 1$ vector, $\mathbf{v}_N$, by taking the last $N-1$ columns of $H(\mathbf{v}_N)$ as

$$HE(\mathbf{v}_N) = H(\mathbf{v}_N)_{:,2:N}. \qquad (2.18)$$

The three operations jointly generate eleven matrix codebooks from vector codebooks as listed in **Table 2.4**. **Table 2.4** contains the operations to generate codebooks $V(N_t, S, L)$ for $N_t = 2, 3, 4$, $S = 2, 3, 4$, and $L = 3, 6$. The set notation $V(N_t, 1, L)$ in the input arguments of the operations denotes that each vector in the codebook $V(N_t, 1, L)$ is sequentially taken as an input to the operations. The output of the operation with one or more codebooks as input arguments is also a codebook.

Table 2.4: Operations to generate codebooks $V(N_t, S, L)$ for $N_t = 2, 3, 4$, $S = 2, 3, 4$, and $L = 3, 6$

$N_t, L \backslash S$	2	3	4
2,3	$H(V(2,1,3))$	-------	-------
3,3	$HE(V(3,1,3))$	$H(V(3,1,3))$	-------
4,3	-------	$HE(V(4,1,3))$	$H(V(4,1,3))$
2,6	$H(V(2,1,6))$	-------	-------
3,6	$HC(V(3,1,3), V(2,1,3))$	$HC(V(3,1,3), H(V(2,1,3)))$	-------
4,6	$HC(V(4,1,3), V(3,1,3))$	$HE(V(4,1,6))$	$H(V(4,1,6))$

2.4 Summary

In this chapter, the limited feedback MIMO system is introduced. The receiver feeds back the index of the optimal precoder which is selected by the proposed precoder selection criteria to the transmitter. The transmitter does not need to know the current CSI. For linear receivers, three precoder selection criteria, Capacity-SC, MSE-SC, and MSV-SC are proposed to select the optimal precoder based on current CSI. Different precoder selection criteria can be chosen according to the system requirements. IEEE 802.16-2005 standard supports the limited feedback MIMO precoding scheme and the codebooks with different dimensions and sizes are also defined in this standard.

Chapter 3

Single-Mode Limited Feedback Precoding for MISO Systems

Limited feedback precoding for MIMO system is a popular technique used to improve system reliability for wireless communications. The single-mode limited feedback system is a system that has only one codebook. In general, the average feedback rate of the limited feedback system is fixed in a transmission. Under this condition, the performance of the single-mode limited feedback system is affected by the codebook size and the variation of the channel.

In the practical communication system, the transmitter has multiple antennas and the receiver generally has only one antenna. Obviously, it is a MISO communication system. The transmit beamforming is a powerful technique for enhancing the MISO system performance. With perfect CSI, the transmit beamforming can achieve optimal performance in the MISO system in terms of maximizing the received SNR [11]-[13].

In Chapter 3, single-mode limited feedback systems are presented first. We consider the transmit beamforming scheme and MISO channel model in this thesis. The channel characteristics are modeled by the first-order Markov channel model. Then the transmit beamforming codebooks in IEEE 802.16-2005 standard are given and used in the computer simulation. Finally, the simulation results are illustrated and discussed.

3.1 Single-Mode Limited Feedback Systems

The single-mode limited feedback system is a system that has only one codebook, either large-size or small-size. Under a fixed average feedback rate, the system with a small-size codebook feeds back less bits more often and that with a large-size codebook feeds back more bits less often. For example, if the average feedback rate is fixed at three bits per frame, the receiver with a 3-bit codebook feeds back three bits **per frame** and that with a 6-bit codebook feeds back six bits **per two frames**. **Figure 3.1** illustrates the single-mode limited feedback system architecture in the MIMO channel.
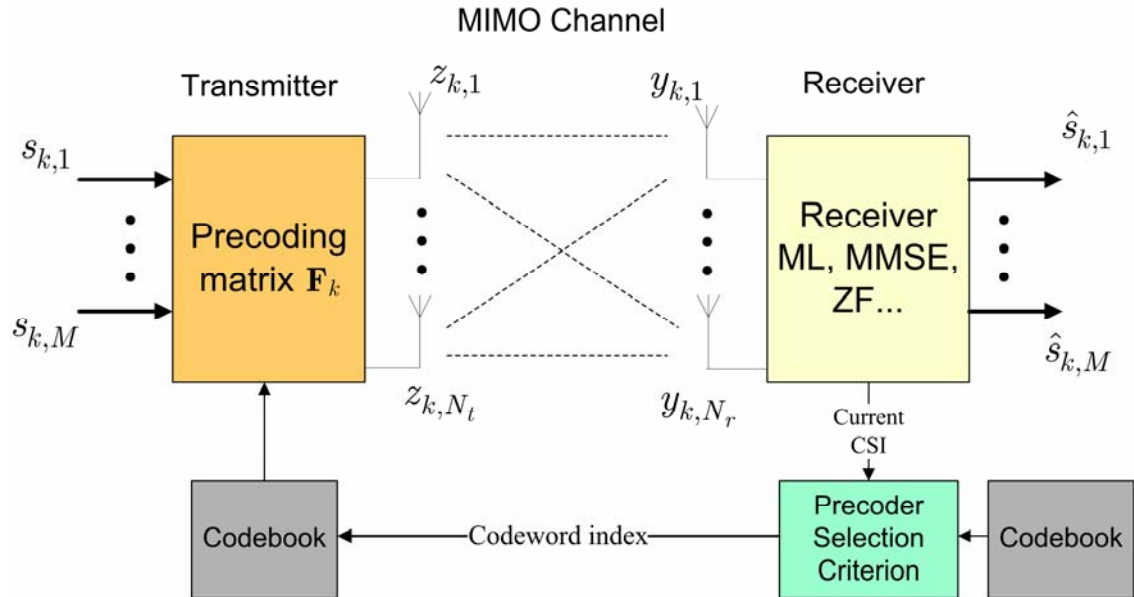
Figure 3.1: Single-mode limited feedback system architecture

Because the receiver generally has only one receive antenna in the practical communication system, we consider the MISO channel model and the transmit beamforming scheme in this thesis. In this section, we will introduce the first-order Markov MISO channel model which is assumed in this thesis. The decoding scheme of the single-mode limited feedback MISO system will be given in the following.

3.1.1 First-Order Markov MISO Channel Model

Consider a MISO channel model with N_t transmit antennas and single receive antenna. In the frame-based transmission, let h_j^k denotes the channel coefficient between the jth transmit antenna and the receive antenna. k is the frame index. We collect h_j^k's into the channel vector $\mathbf{h}_k = \left[h_1^k, h_2^k, ..., h_{N_t}^k\right]$. $\mathbf{f}_k$ is the beamformer and g_k is the gain control factor for the kth frame. $\mathbf{s}_k$ is the $1 \times L$ data symbol vector and $\hat{\mathbf{s}}_k$ is the $1 \times L$ detected symbol vector for the kth frame, where L is the frame length. We assume that $\mathbf{E}_{\mathbf{s}_k}\left[\mathbf{s}_k \mathbf{s}_k^H\right] = \mathbf{I}_L$ for power constraint reasons. The transmit beamforming for MISO system is illustrated in **Figure 3.2**.
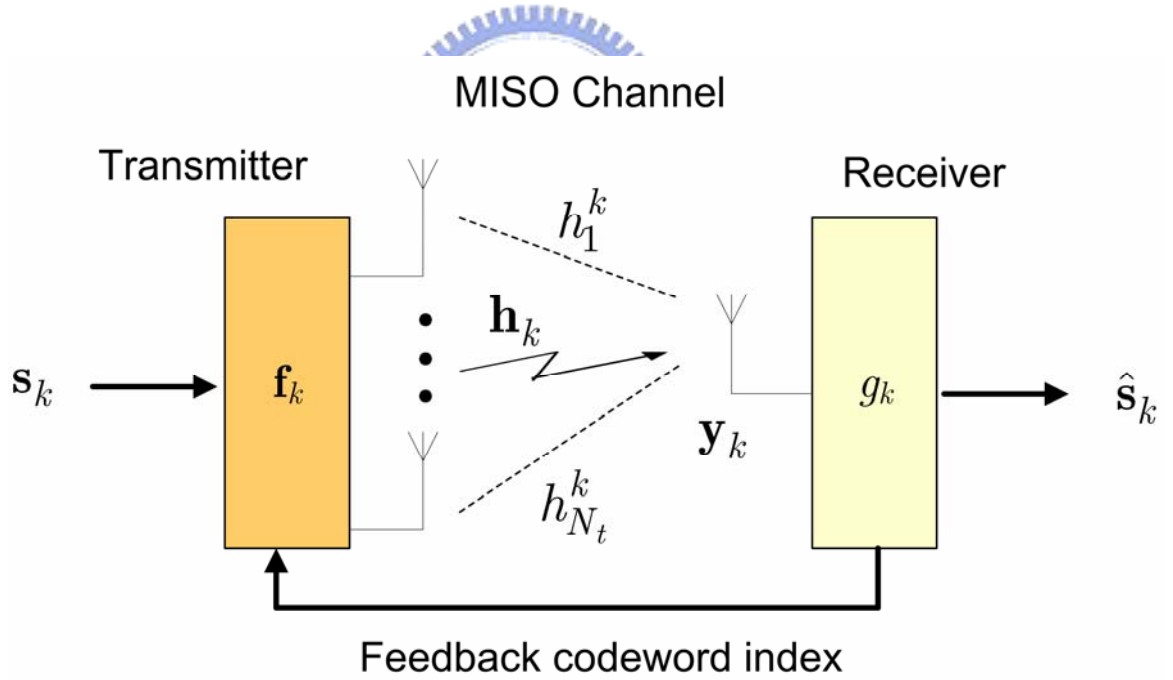
Figure 3.2: Transmit beamforming scheme for MISO system

The data symbol vector $\mathbf{s}_k$ is multiplied by an $N_t \times 1$ beamformer $\mathbf{f}_k$ which is selected as a function of the current CSI by using the proposed beamformer selection criterion. Assuming perfect timing, synchronization, and sampling, the discrete-time

equivalent received signal can be written as

$$\mathbf{y}_k = \mathbf{h}_k \mathbf{f}_k \mathbf{s}_k + \mathbf{n}_k, \tag{3.1}$$

where $\mathbf{h}_k$ is the $1 \times N_t$ channel vector and $\mathbf{n}_k$ is the $1 \times L$ noise vector for the k th frame. The entries of $\mathbf{n}_k$ are independent and distributed according to $\mathcal{CN}\left(0, \sigma_n^2\right)$. We assume that the channel is quasi-static in a frame period and all elements of $\mathbf{h}_k$ are independent identically distributed (i.i.d.) according to a complex Gaussian distribution with zero-mean and unit variance; that is

$$\mathbf{h}_k \sim \mathcal{CN}\left(\mathbf{0}, \mathbf{I}_{N_t}\right). \tag{3.2}$$

The time-varying property of the MISO channel can be characterized by the first-order Markov channel model. The first-order Markov channel model is only characterized by the one-tap temporal-correlation coefficient ρ. The channel vector for the $(k+1)$ th frame is given by

$$\mathbf{h}_{k+1} = \sqrt{\rho}\mathbf{h}_k + \Delta\mathbf{h}, \tag{3.3}$$

where k is the frame index, $\Delta\mathbf{h} \sim \mathcal{CN}\left(\mathbf{0}, (1-\rho)\mathbf{I}_{N_t}\right)$, and ρ is the temporal-correlation coefficient ($0 \le \rho \le 1$). A small $\rho (= 0)$ implies the fast fading environment and a large $\rho (= 1)$ corresponds to the time-invariant channel. The feature of the first-order Markov channel model is that the channel can be characterized by only one-tap temporal-correlation coefficient. The channel can be modeled as a time-invariant channel with a large ρ or a time-varying channel with a small ρ. This channel model is also widely used in other research papers [13],[28]-[31].

3.1.2 Decoding Scheme of Limited Feedback MISO Systems

In MISO systems, linear receivers apply a gain control factor g_k to produce the hard decoded symbol vector $\hat{\mathbf{s}}_k$, where $\hat{\mathbf{s}}_k = g_k \mathbf{y}_k$. For a zero-forcing linear receiver, the gain control factor g_k is defined as

$$g_k = \left(\mathbf{h}_k \mathbf{f}_k\right)^+, \tag{3.4}$$

where $(\cdot)^+$ is the matrix pseudo-inverse, $\mathbf{h}_k$ is the $1 \times N_t$ channel vector, and $\mathbf{f}_k$ is the $N_t \times 1$ transmit beamformer. The hard decoded symbol vector $\hat{\mathbf{s}}_k$ from the ZF decoder can be written as

$$\hat{\mathbf{s}}_k = g_k \mathbf{y}_k = \left(\mathbf{h}_k \mathbf{f}_k\right)^+ \mathbf{h}_k \mathbf{f}_k \mathbf{s}_k + \left(\mathbf{h}_k \mathbf{f}_k\right)^+ \mathbf{n}_k = \underbrace{\mathbf{s}_k}_{\text{signal}} + \underbrace{\left(\mathbf{h}_k \mathbf{f}_k\right)^+ \mathbf{n}_k}_{\text{noise}}. \tag{3.5}$$

The decoded symbol vector $\hat{\mathbf{s}}_k$ will be fed into the demodulator and the decoded binary data stream will be produced from the demodulator.

When the transmitter is precoded with the beamformer $\mathbf{f}_k$, the equivalent channel is $\mathbf{h}_k \mathbf{f}_k$. $\mathbf{h}_k$ is the $1 \times N_t$ channel vector and $\mathbf{f}_k$ is the $N_t \times 1$ beamformer. Actually, $\mathbf{h}_k \mathbf{f}_k$ is a received power gain provided by the channel and the beamformer. The larger the received power gain is, the better the system performance is. The beamformer selection criterion is stated as follows:

Maximum Signal-to-Noise Ratio Selection Criterion (MSNR-SC):

Pick $\mathbf{f}_k$ such that

$$\mathbf{f}_k = \arg \max_{\mathbf{f}_i \in \mathcal{F}} \left|\mathbf{h}_k \mathbf{f}_i\right|^2, \tag{3.6}$$

where $\mathcal{F}$ is the beamformer set and $|\cdot|^2$ is the square of the vector norm. The transmit beamforming scheme can increase the received power gain and improve the system performance.

3.2 Transmit Beamforming Codebooks in IEEE 802.16-2005

IEEE 802.16-2005 standard [25] supports the limited feedback MIMO precoding scheme. The transmit beamforming is a special case of the MIMO precoding with $M = 1$ and $N_r = 1$, where M is the number of substreams and N_r is the number of receive antennas. In this standard, all codebooks are divided into two kinds: 3-bit codebooks and 6-bit codebooks. The transmit beamforming ($M = 1$) codebooks are listed in **Table 3.1**. The notation $V(N_t, S, L)$ denotes the vector codebook, which consists of 2^L complex, unit vectors of a dimension N_t. S denotes the number of substreams. All the codewords of $V(2,1,3)$, $V(3,1,3)$, and $V(4,1,3)$ are listed in **Table 2.1**, **Table 2.2**, and **Table 2.3**.

Table 3.1: Transmit beamforming codebooks in IEEE 802.16-2005 standard

$N_t, S \setminus L$	**3**	**6**
2,1	$V(2,1,3)$	$V(2,1,6)$
3,1	$V(3,1,3)$	$V(3,1,6)$
4,1	$V(4,1,3)$	$V(4,1,6)$

In IEEE 802.16-2005 standard [25], two vector codebooks $V(3,1,6)$ and $V(4,1,6)$ are generated as follows. All the vector codewords $\mathbf{v}_i$, $i = 2,...,2^L$ are derived from the first codeword $\mathbf{v}_1$ as

$$\tilde{\mathbf{v}}_i = H(\mathbf{s})Q^i(\mathbf{u})H^H(\mathbf{s})\mathbf{v}_{i-1}, \quad \text{for } i = 2,..,2^L, \tag{3.7}$$

$$\mathbf{v}_i = \tilde{\mathbf{v}}_i e^{-j\phi_1}, \quad \text{for } i = 2,..,2^L, \tag{3.8}$$

where $Q^i(\mathbf{u}) = \mathrm{diag}\left(e^{j\cdot\frac{2\pi}{2^L}\cdot u_1\cdot i},...,e^{j\cdot\frac{2\pi}{2^L}\cdot u_{N_t}\cdot i}\right)$ is a diagonal matrix, $\mathbf{u} = \left[u_1,...,u_{N_t}\right]$ is

an interger vecror, $\mathbf{v}_1 = \frac{1}{\sqrt{N_t}}\left[1,e^{j\cdot\frac{2\pi}{N_t}},...,e^{j\cdot\frac{2\pi}{N_t}(N_t-1)}\right]^T$, and ϕ_i is the phase of the

first entry of $\tilde{\mathbf{v}}_i$. $H(\cdot)$ is defined in the Equation (2.16). The parameters for the

generation of $V(3,1,6)$ and $V(4,1,6)$ are listed in **Table 3.2** and the codewords of

$V(3,1,6)$ is listed in **Table 3.3**.

Table 3.2: Generating parameters for $V(3,1,6)$ and $V(4,1,6)$

N_t	L	$\mathbf{u}$ in $Q^i(\mathbf{u})$	$\mathbf{s}$ in $H(\mathbf{s})$
3	6	$[1,26,57]$	$[1.2518 - j0.6409, -0.4570 - j0.4974, 0.1177 + j0.2360]^T$
4	6	$[1,45,22,49]$	$[1.3954 - j0.0738, 0.0206 + j0.4326,$ $-0.1658 - j0.5445, 0.5487 - j0.1599]^T$

We can follow the above algorithms to generate the vector codebooks $V(3,1,6)$

and $V(4,1,6)$. Unfortunately, IEEE 802.16-2005 standard does not provide the

generating parameters for the codebook $V(2,1,6)$.

The 6-bit codebook provides sixty-four beamformers to be selected. It has higher

probability that the optimal beamformer which is closest to the unquantized optimal

beamformer can be selected. But the receiver needs to feed back six bits in a

transmission. Although the 3-bit codebook provides only eight beamformers to be

selected, the receiver needs to feed back only three bits in a transmission.

Table 3.3: MIMO precoding codebook $V(3,1,6)$

Matrix index (binary)	Column 1	Matrix index (binary)	Column 1
000000	0.5774	100000	0.5437
	−0.2887 + j0.5000		−0.1363 − j0.4648
	−0.2887 − j0.5000		0.4162 + j0.5446
000001	0.5466	100001	0.5579
	0.2895 − j0.5522		−0.6391 +j0.3224
	0.2440 + j0.5030		−0.2285 − j0.3523
000010	0.5246	100010	0.5649
	−0.7973 − j0.0214		0.6592 − j0.3268
	−0.2517 − j0.1590		0.1231 + j0.3526
000011	0.5973	100011	0.484
	0.7734 + j0.0785		−0.6914 − j0.3911
	0.1208 + j0.1559		−0.3669 +j0.0096
000100	0.4462	100100	0.6348
	−0.3483 − j0.6123		0.5910 + j0.4415
	−0.5457 + j0.0829		0.2296 − j0.0034
000101	0.6662	100101	0.4209
	0.2182 + j0.5942		0.0760 − j0.5484
	0.3876 − j0.0721		−0.7180 +j0.0283
000110	0.412	100110	0.6833
	0.3538 − j0.2134		−0.1769 +j0.4784
	−0.8046 − j0.1101		0.5208 − j0.0412
000111	0.684	100111	0.4149
	−0.4292 + j0.1401		0.3501 + j0.2162
	0.5698 + j0.0605		−0.7772 − j0.2335
001000	0.4201	101000	0.6726
	0.1033 + j0.5446		−0.4225 − j0.2866
	−0.6685 − j0.2632		0.5061 + j0.1754
001001	0.6591	101001	0.419
	−0.1405 − j0.6096		−0.2524 + j0.6679
	0.3470 + j0.2319		−0.5320 − j0.1779
001010	0.407	101010	0.6547
	−0.5776 + j0.5744		0.2890 − j0.6562
	−0.4133 + j0.0006		0.1615 + j0.1765

Table 3.3: MIMO precoding codebook $V(3,1,6)$ (continued)

Matrix index (binary)	Column 1	Matrix index (binary)	Column 1
001011	0.6659	101011	0.3843
	0.6320 – j0.3939		–0.7637 + j0.3120
	0.0417 + j0.0157		–0.3465 + j0.2272
001100	0.355	101100	0.69
	–0.7412 – j0.029		0.6998 + j0.0252
	–0.3542 + j0.445		0.0406 – j0.1786
001101	0.7173	101101	0.3263
	0.4710 + j0.3756		–0.4920 – j0.3199
	0.1394 – j0.3211		–0.4413 + j0.5954
001110	0.307	101110	0.7365
	–0.0852 – j0.414		0.0693 + j0.4971
	–0.5749 + j0.629		0.2728 – j0.3623
001111	0.74	101111	0.3038
	–0.3257 + j0.346		0.3052 – j0.2326
	0.3689 – j0.3007		–0.6770 + j0.5496
010000	0.3169	110000	0.727
	0.4970 + j0.1434		–0.5479 – j0.0130
	–0.6723 + j0.424		0.3750 – j0.1748
010001	0.7031	110001	0.3401
	–0.4939 – j0.429		0.4380 + j0.5298
	0.2729 – j0.0509		–0.5470 + j0.3356
010010	0.3649	110010	0.6791
	0.1983 + j0.7795		–0.1741 – j0.7073
	–0.3404 + j0.3224		0.0909 – j0.0028
010011	0.6658	110011	0.3844
	0.2561 – j0.6902		–0.1123 + j0.8251
	–0.0958 – j0.0746		–0.1082 + j0.3836
010100	0.3942	110100	0.6683
	–0.3862 + j0.6614		0.5567 – j0.3796
	0.0940 + j0.4992		–0.2017 – j0.2423
010101	0.6825	110101	0.394
	0.5632 + j0.0490		–0.5255 + j0.3339
	–0.1901 – j0.4225		0.2176 + j0.6401

Table 3.3: MIMO precoding codebook $V(3,1,6)$ (continued)

Matrix index (binary)	Column 1	Matrix index (binary)	Column 1
010110	0.3873	110110	0.6976
	−0.4531 − j0.0567		0.2872 + j0.3740
	0.2298 + j0.7672		−0.0927 − j0.5314
010111	0.7029	110111	0.3819
	−0.1291 + j0.4563		−0.1507 − j0.3542
	0.0228 − j0.5296		0.1342 + j0.8294
011000	0.387	111000	0.6922
	0.2812 − j0.3980		−0.5051 + j0.2745
	−0.0077 + j0.7828		0.0904 − j0.4269
011001	0.6658	111001	0.4083
	−0.6858 − j0.0919		0.6327 − j0.1488
	0.0666 − j0.2711		−0.0942 + j0.6341
011010	0.4436	111010	0.6306
	0.7305 + j0.2507		−0.5866 − j0.4869
	−0.0580 + j0.4511		−0.0583 − j0.1337
011011	0.5972	111011	0.4841
	−0.2385 − j0.7188		0.5572 + j0.5926
	−0.2493 − j0.0873		0.0898 + j0.3096
011100	0.5198	111100	0.5761
	0.2157 + j0.7332		0.1868 − j0.6492
	0.2877 + j0.2509		−0.4292 − j0.1659
011101	0.571	111101	0.5431
	0.4513 − j0.3043		−0.1479 + j0.6238
	−0.5190 − j0.3292		0.4646 + j0.2796
011110	0.5517	111110	0.5764
	−0.3892 + j0.3011		0.4156 + j0.1263
	0.5611 + j0.3724		−0.4947 − j0.4840
011111	0.5818	111111	0.549
	0.1190 + j0.4328		−0.3963 − j0.1208
	−0.3964 − j0.5504		0.5426 + j0.4822

3.3 Computer Simulations

In IEEE 802.16-2005 standard [25], all codebooks can be divided into two kinds: 3-bit codebooks and 6-bit codebooks. Under a fixed average feedback rate, two modes are defined as follows: (1) Mode I is defined in which the transmitter is precoded with the 6-bit beamformer and the receiver feeds back six bits **per two frames**; (2) Mode II is defined in which the transmitter is precoded with the 3-bit beamformer and the receiver feeds back three bits **per frame**. The schemes of Mode I and Mode II are illustrated in **Figure 3.3**.
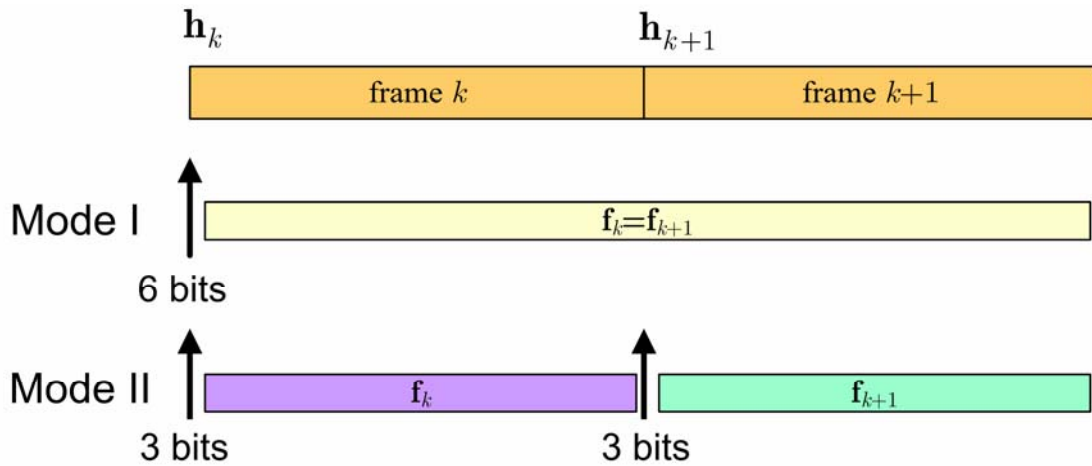
Figure 3.3: Transmit beamforming schemes of Mode I and Mode II

In the following, we illustrate the performances of the single-mode limited feedback MISO system. Besides, we also consider a MISO-OFDM system in the simulations and illustrate the performances of the single-mode limited feedback MISO-OFDM system. Under a fixed average feedback rate at three bits per frame or per OFDM symbol period, the schemes of Mode I and Mode II for single-carrier systems and multi-carrier systems are commented in **Table 3.4**.

Table 3.4: Schemes of Mode I and Mode II for single-carrier and multi-carrier systems

Fixed average feedback rate at 3 bits/frame (or OFDM symbol period)		
	Single-Carrier (MISO)	**Multi-Carrier (MISO-OFDM)**
Mode I	feed back 6 bits per two frames	feed back 6 bits per tone and per two OFDM symbol periods
Mode II	feed back 3 bits per frame	feed back 3 bits per tone and per OFDM symbol period

(a) Single-mode limited feedback MISO system

   Table 3.5 lists all parameters used in this simulation. This simulation uses 16-QAM modulation and one data substream on a 4×1 wireless system. The transmit beamforming codebooks in IEEE 802.16-2005 are applied in the simulation. The average feedback rate is fixed at three bits per frame. In Mode I, the receiver feeds back six bits to the transmitter **per two frames**; in Mode II, the receiver feeds back three bits to the transmitter **per frame**. Each frame consists of 128 symbols and each transmission consists of 16 frames.

   The channel is assumed to be quasi-static and Rayleigh fading. The channel gains of two consecutive frames follow the first-order Markov channel model (Equation (3.3)). The elements of the random perturbation $\Delta \mathbf{h}$ in Equation (3.3) are assumed to be independent identically distributed (i.i.d.) complex Gaussian random variables with zero-mean and variance $(1 - \rho)$. SNR is defined as the ratio of the average received signal power to the average received noise power. Perfect channel knowledge known at the receiver and the error-free feedback channel are also assumed in the simulation. SER performances of the single-mode limited feedback MISO system (operating in Mode I or Mode II) with $\rho = 1, 0.9, 0.8, 0.7$ are shown in Figures 3.4-3.7.

Table 3.5: Simulation environment of the single-mode limited feedback MISO system

Parameter	Values
Channel	Rayleigh fading channel (First-order Markov channel model)
Modulation	16-QAM
Number of transmit antenna	4
Number of receive antenna	1
Fixed average feedback rate	3 bits per frame
Frame length	128 symbols
Number of frames	16 frames per transmission
Codebook	Transmit beamforming codebooks in IEEE 802.16-2005

When $\rho = 1$, **Figure 3.4** illustrates that the SER performance of Mode I (6-bit beamformer) is better than that of Mode II (3-bit beamformer). The channel does not vary in the two consecutive frame periods. In Mode I, the optimal beamformer can be selected from the 6-bit codebook (sixty-four beamformers) at the start of the first frame of the two consecutive frames, and it is also optimal for the channel of the second frame. In Mode II, the optimal beamformer is selected from the 3-bit codebook (eight beamformers) at the start of the first frame, and it can be reselected at the start of the second frame. Because the optimal beamformer selected from the 6-bit codebook is closer to the unquantized optimal beamformer than that selected from the 3-bit codebook, the SER performance of Mode I is better than that of Mode II.
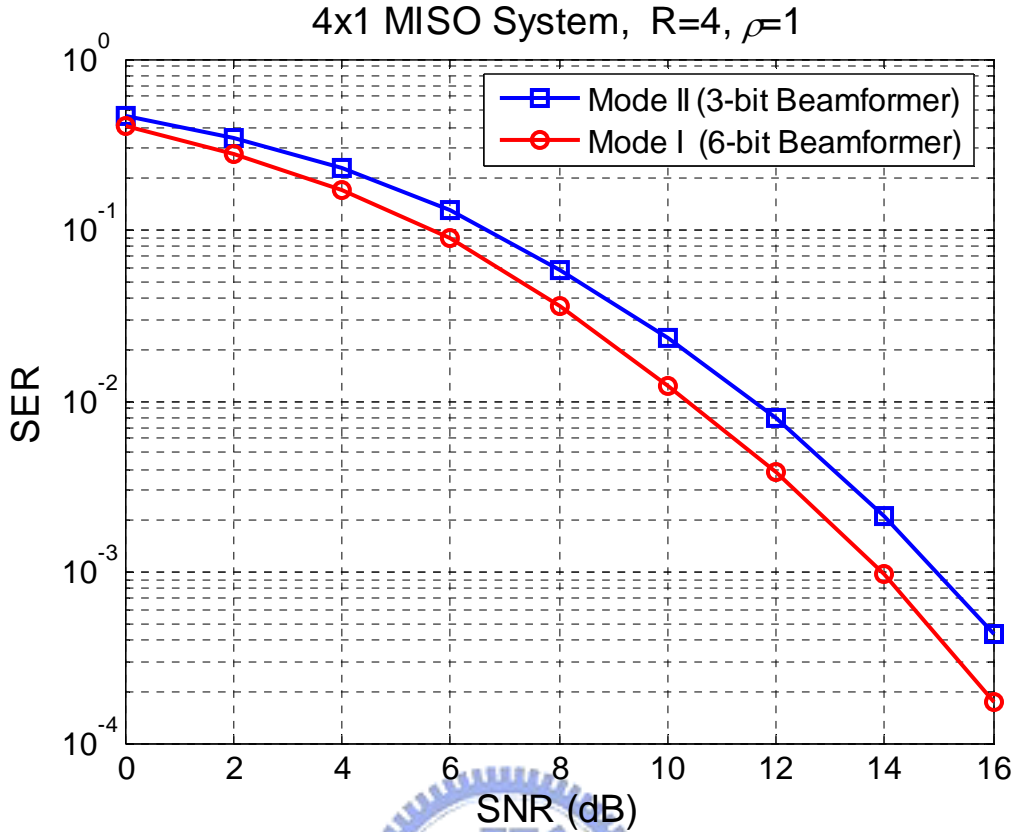
Figure 3.4: SER performance of the single-mode 4×1 MISO system with $\rho = 1$

When $\rho = 0.9$, **Figure 3.5** illustrates that the SER performance of Mode I becomes slightly poorer than that in **Figure 3.4**. The curve of Mode I crosses the curve of Mode II at SNR=14 dB. When $\rho = 0.8$, **Figure 3.6** shows that the SER performance of Mode I becomes poorer than that in **Figure 3.5**. The curve of Mode I crosses the curve of Mode II at SNR=10 dB. When $\rho = 0.7$, **Figure 3.7** shows that the SER performance of Mode II is better than that of Mode I.

The reason that the SER performance of Mode I becomes poorer as ρ decreases is that the beamformer which is optimal for the channel of the k th frame is not always optimal for that of the $(k+1)$ th frame. The nonoptimal beamformer decreases the average received power gain over the $(k+1)$ th frame. The single-mode system operating in Mode I loses diversity gain as ρ decreases.
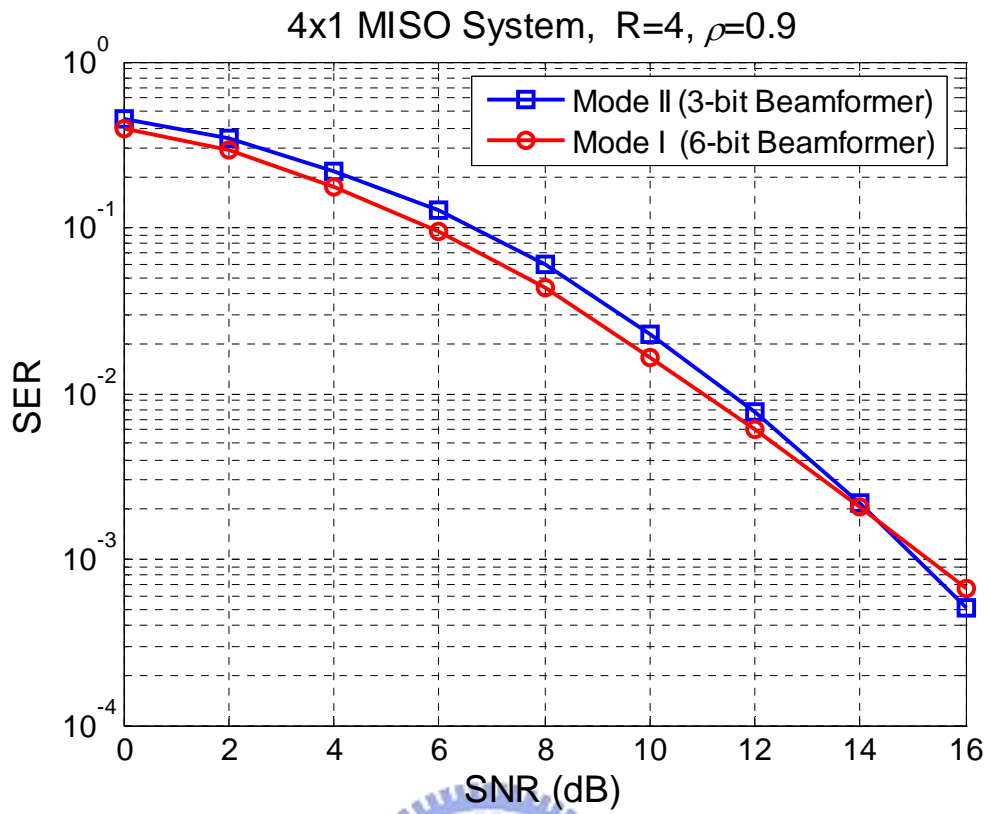
Figure 3.5: SER performance of the single-mode 4×1 MISO system with $\rho = 0.9$
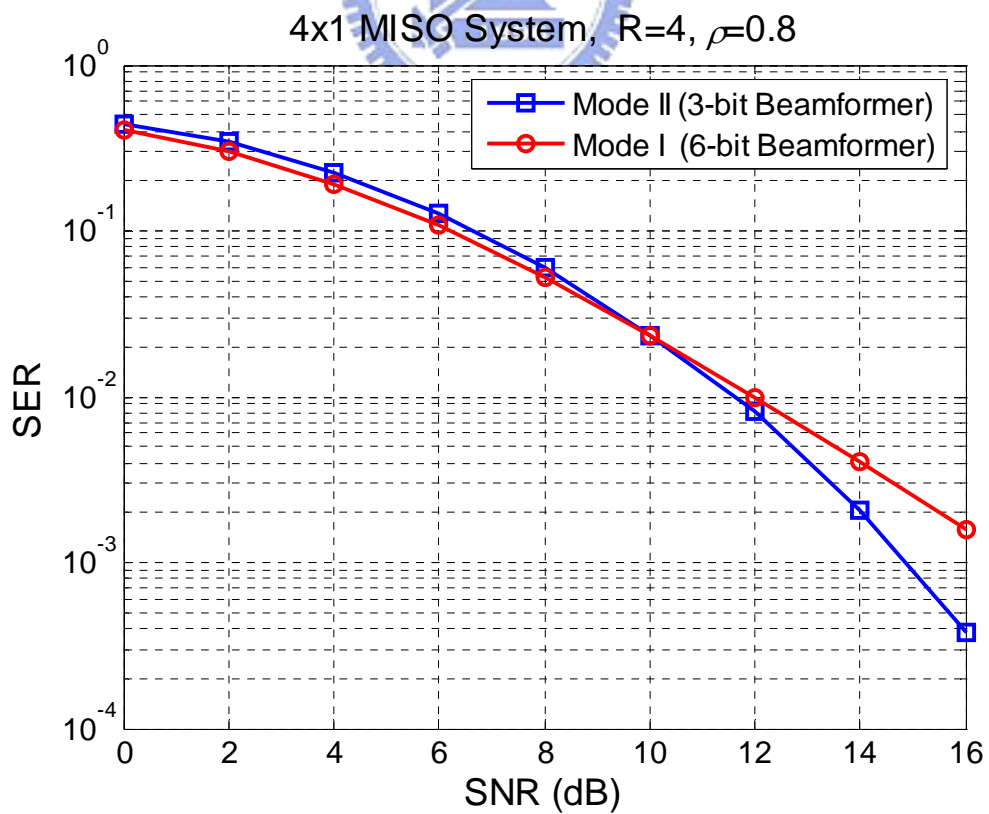
Figure 3.6: SER performance of the single-mode 4×1 MISO system with $\rho = 0.8$
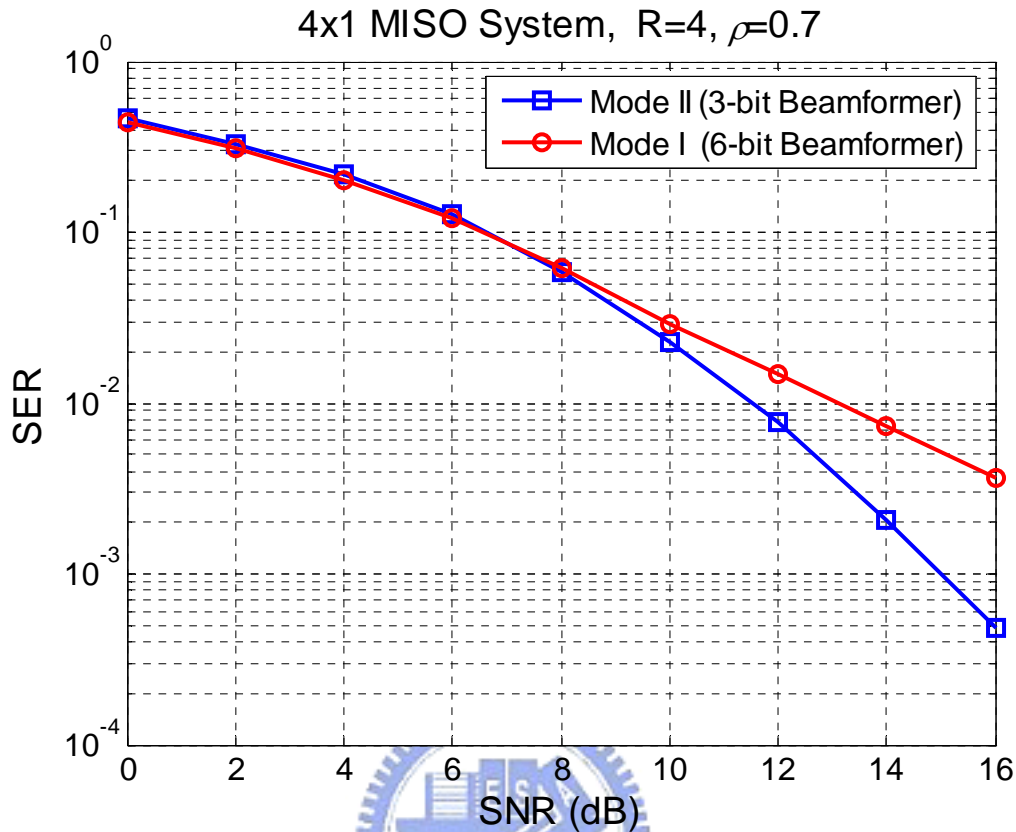
Figure 3.7: SER performance of the single-mode 4×1 MISO system with $\rho = 0.7$

Figure 3.8 shows the SER performance comparison between Mode I and Mode II under a fixed SNR=12 dB. The two lines cross at about $\rho = 0.85$. **Figure 3.8** shows that when the channel is subject to high temporal correlation $(\rho \geq 0.85)$, Mode I outperforms Mode II whereas with $\rho < 0.85$ the latter yields better performance. It is obviously observed that Mode I is suitable to be used in the high temporal-correlation channel and Mode II is suitable to be used in the low temporal-correlation channel. From the simulation results, we observed that the single-mode limited feedback system (either Mode I or Mode II) is not robust enough in mobile environments.
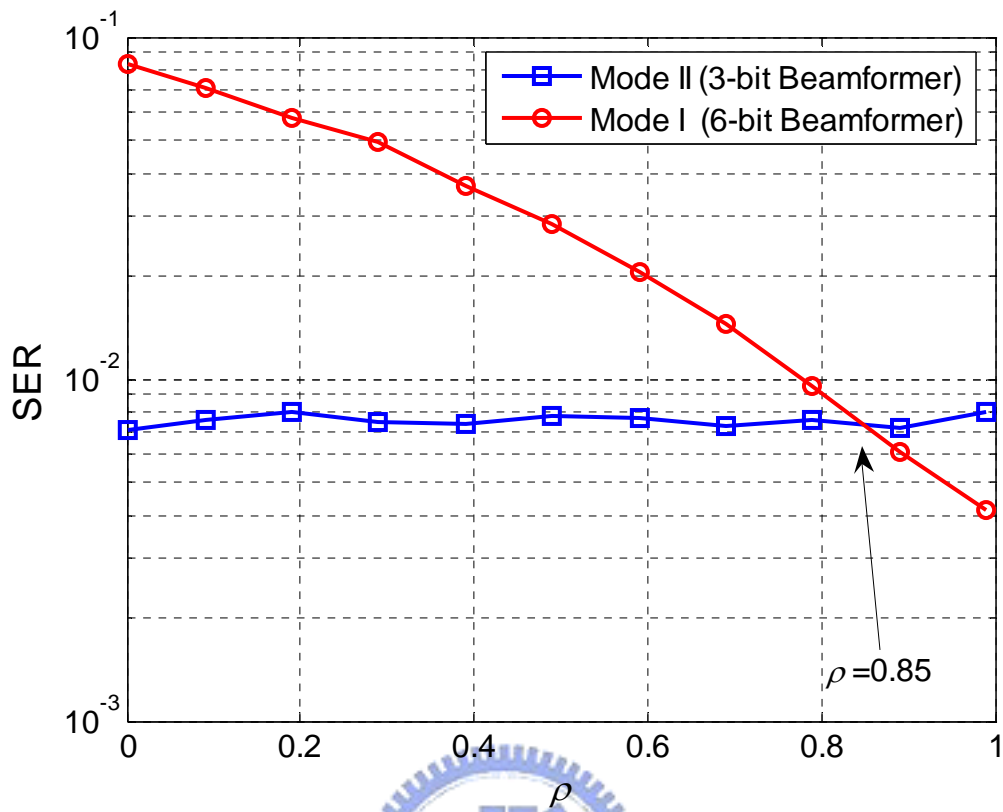
Figure 3.8: SER performance comparison between Mode I and Mode II for 4×1

MISO system

(b) Single-mode limited feedback MISO-OFDM system

We consider a MISO-OFDM system and **Table 3.6** lists all parameters used in this simulation. This simulation uses 16-QAM modulation and 128 subcarriers in the MISO-OFDM system. The multipath Rayleigh fading channel is used in the simulation. The channel gains of two consecutive OFDM symbol periods follow the first-order Markov channel model (Equation (3.3)), and the relative delays and the average power follow the parameters of the channel model defined in ITU-R M.1225 [37]. The elements of the random perturbation $\Delta \mathbf{h}$ in Equation (3.3) are assumed to be i.i.d. zero-mean complex Gaussian with variance $(1 - \rho)$. SNR is defined as the ratio of the average received signal power to the average received noise power after DFT. Perfect channel knowledge known at the receiver and the error-free feedback channel are also assumed in the simulation.

The parameters of the simulation environment of the MISO-OFDM system follow IEEE 802.16-2005 [25] and are stated as follows: The FFT length is 128. The bandwidth is 2.5MHz and the sampling frequency is 2.8 MHz. The sampling time is 357.14 ns and the subcarrier spacing is 21.875 kHz. The ratio of CP time is 1/4. The OFDM symbol time is 57.143 us. Each frame consists of 16 OFDM symbols.

The transmit beamforming codebooks in IEEE 802.16-2005 are applied in the simulation. The average feedback rate is fixed at three bits per tone and per OFDM symbol period. In Mode I, the receiver feeds back six bits to the transmitter **per tone and per two OFDM symbol periods**; in Mode II, the receiver feeds back three bits to the transmitter **per tone and per OFDM symbol period**. The transmit symbols are precoded with the beamformers tone by tone and we assume that all subcarriers are independent. SER performances of the single-mode limited feedback MISO-OFDM systems with $\rho = 1, 0.9, 0.8, 0.7$ are shown in Figures 3.9-3.12.

Table 3.6: Simulation environment of the single-mode limited feedback MISO-OFDM system

Parameter	Values					
Channel	Multipath Rayleigh fading channel (First-order Markov channel model)					
Tap (ITU-R M.1225)	1	2	3	4	5	6
Relative delay (ns)	0	310	710	1090	1730	2510
Average power (dB)	0	-1	-9	-10	-15	-20
Bandwidth	2.5 MHz					
FFT length	128					
Sampling frequency	2.8 MHz					
Subcarrier spacing	21.875 kHz					
Useful symbol time	45.714 us					
Ratio of CP time	1/4					
CP time	11.429 us					
Symbol time	57.143 us					
Sampling time	357.14 ns					
Frame length	16 OFDM symbols					
Modulation	16-QAM					
Number of transmit antenna	4					
Number of receive antenna	1					
Fixed average feedback rate	3 bits per OFDM symbol period					
Codebook	Transmit beamforming codebooks in IEEE 802.16-2005					

Figure 3.9: SER performance of the single-mode 4×1 MISO-OFDM system with $\rho = 1$

When $\rho = 1$, **Figure 3.9** illustrates that the SER performance of Mode I is also better than that of Mode II in the MISO-OFDM system. The channel does not vary in the two consecutive OFDM symbol periods. In Mode I, the optimal beamformers for all subcarriers can be selected from the 6-bit codebook at the start of the first OFDM symbol of the two consecutive OFDM symbols, and they are also optimal for the channels of the second OFDM symbol time. In Mode II, the optimal beamformers are selected from the 3-bit codebook at the start of the first OFDM symbol, and they will be reselected at the start of the second OFDM symbol. Because the optimal beamformers selected from the 6-bit codebook are closer to the unquantized optimal beamformers for all subcarriers than that selected from the 3-bit codebook, the SER performance of Mode I is always better than that of Mode II.
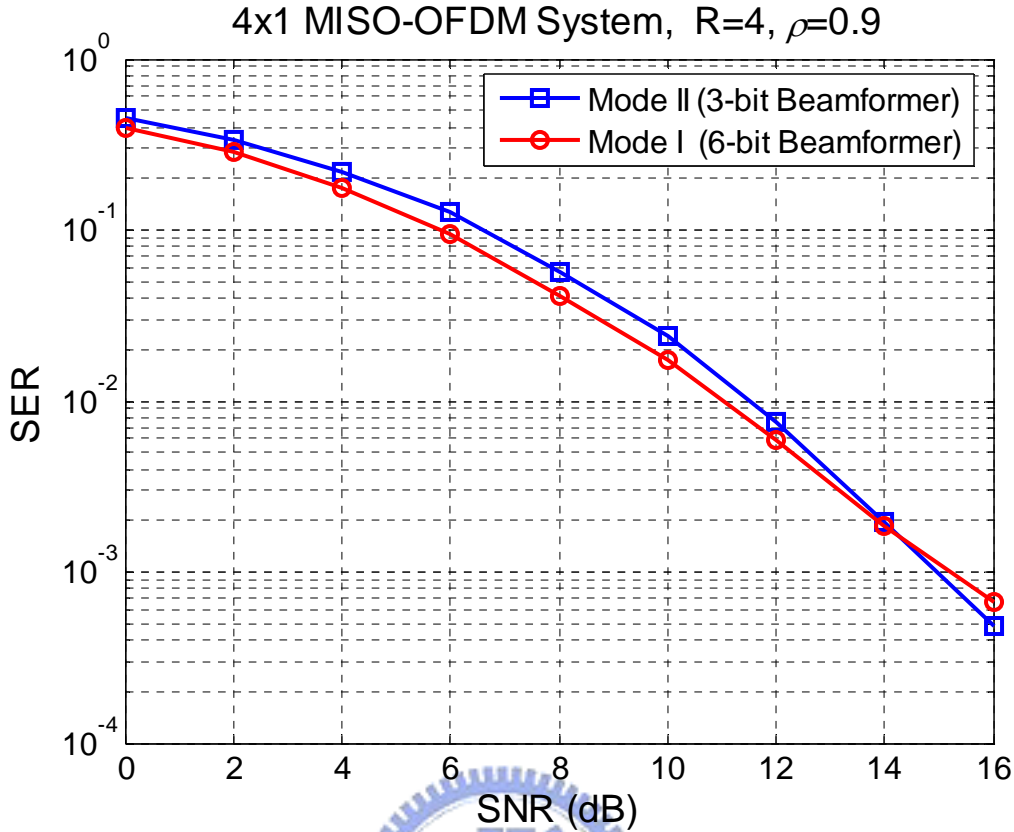
Figure 3.10: SER performance of the single-mode 4×1 MISO-OFDM system with $\rho = 0.9$

When $\rho = 0.9$, **Figure 3.10** illustrates that the SER performance of Mode I also becomes slightly poorer than that in **Figure 3.9**. Two lines cross at SNR=14 dB. When $\rho = 0.8$, **Figure 3.11** shows that the SER performance of Mode I becomes poorer than that in **Figure 3.10**. The curve of Mode I crosses the curve of Mode II at SNR=10 dB. When $\rho = 0.7$, **Figure 3.12** shows that the SER performance of Mode II is better than that of Mode I.

The reason that the SER performance of Mode I becomes poorer as ρ decreases is that the beamformers which are optimal for the channel of the k th OFDM symbol time are not always optimal for the channel of the $(k+1)$ th OFDM symbol time. The nonoptimal beamformers decrease the average received power gain and diversity gain over the $(k+1)$ th OFDM symbol time as ρ decreases.
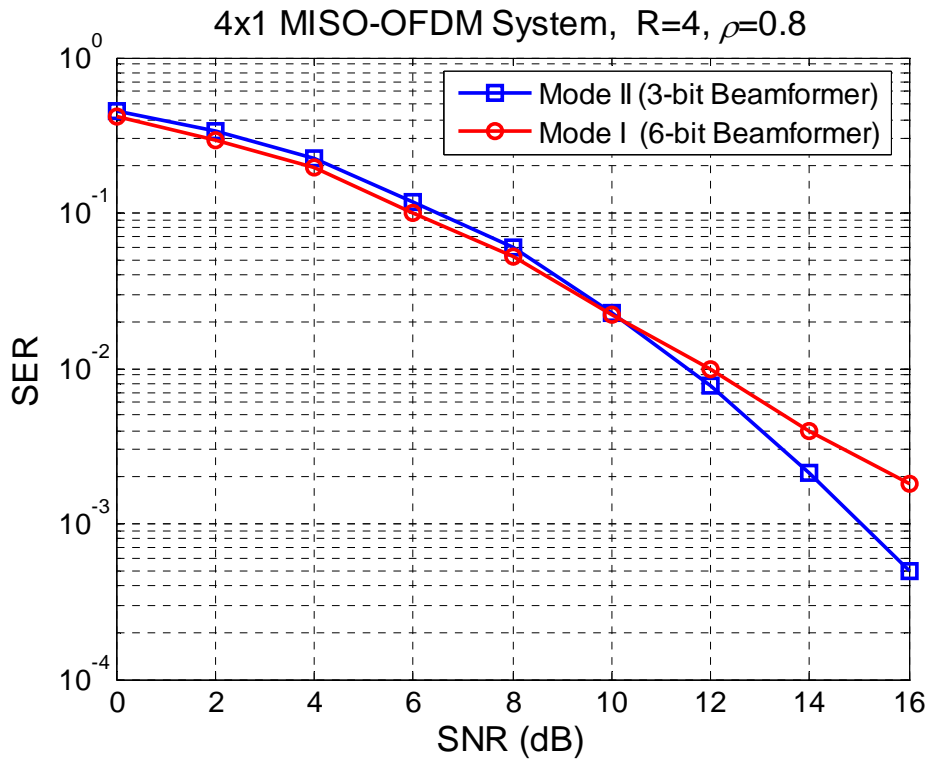
Figure 3.11: SER performance of the single-mode 4×1 MISO-OFDM system with

$\rho = 0.8$
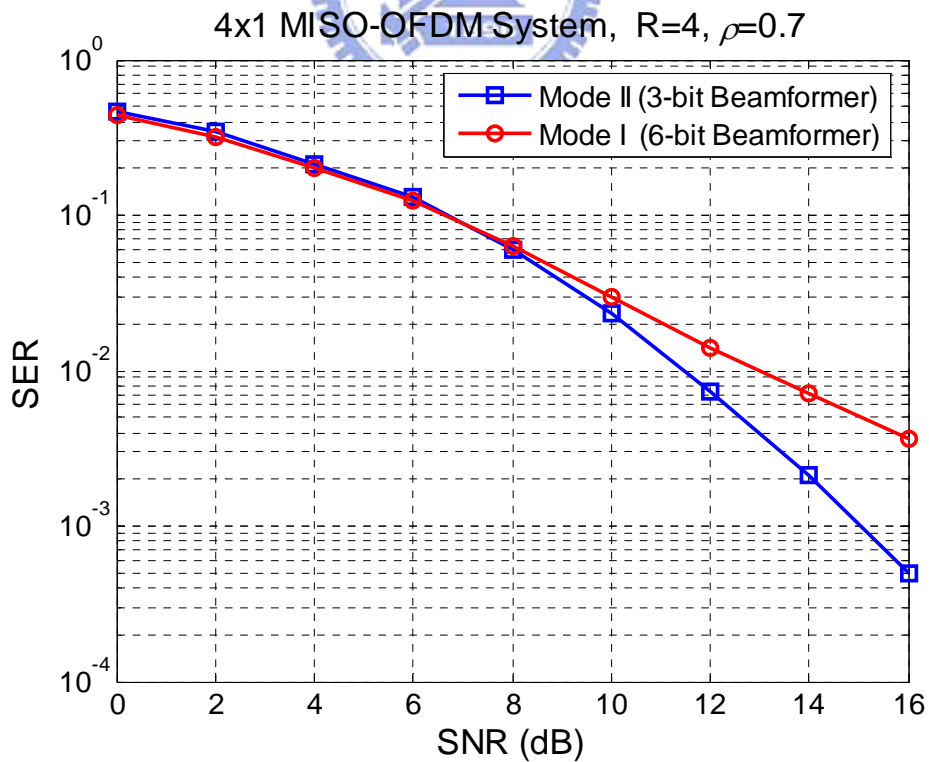
Figure 3.12: SER performance of the single-mode 4×1 MISO-OFDM system with

$\rho = 0.7$
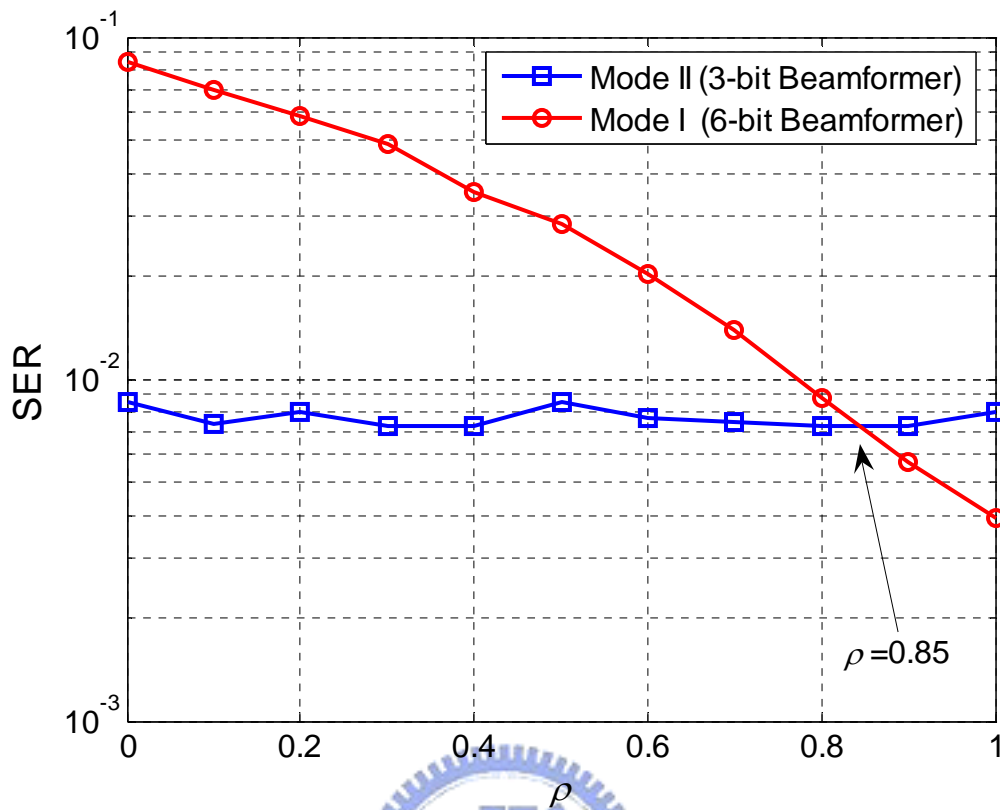
Figure 3.13: SER performance comparison between Mode I and Mode II for

4×1 MISO-OFDM system

Figure 3.13 shows the SER performance comparison between Mode I and Mode II for 4×1 MISO-OFDM system under a fixed SNR=12 dB. Two lines cross at about $\rho = 0.85$. **Figure 3.13** shows that when the channel is subject to high temporal correlation $(\rho \geq 0.85)$, Mode I outperforms Mode II whereas with $\rho < 0.85$ the latter yields better performance.

We compare the above simulation results with that of MISO systems. It is obviously observed that the results of the MISO-OFDM system are similar to that of the MISO system because the multipath channel response can be reduced into a multiplicative constant on a tone-by-tone basis by DFT at the receiver and all subcarriers are independent. The properties of the OFDM system will be given in Chapter 4.

3.4 Summary

The single-mode limited feedback system has been introduced in this chapter. We consider the transmit beamforming scheme and MISO channel model in this thesis and use the first-order Markov channel to model the temporal-correlation channels. The transmit beamforming codebooks in IEEE 802.16-2005 standard are applied in our simulation. The results show that the performance of Mode I becomes poorer as ρ decreases in the MISO system and in the MISO-OFDM system. Obviously, the single-mode limited feedback system is not robust enough in mobile environments. Mode I is suitable to be used in the high temporal-correlation channel and Mode II is suitable to be used in the low temporal-correlation channel.

Chapter 4

Dual-Mode Limited Feedback Precoding for MISO Systems

In Chapter 3, we introduced the single-mode limited feedback precoding for MISO systems. It is obviously observed that the performance of the single-mode limited feedback system is affected by the codebook size and the temporal-correlation coefficient of the channel. Under a fixed average feedback rate, the single-mode limited feedback system is not robust enough in mobile environments. The system with a large-size codebook is suitable to be used in the high temporal-correlation channel and that with a small-size codebook is suitable to be used in the low temporal-correlation channel. To solve this problem, we propose a dual-mode limited feedback system with an SER based mode selection criterion in this chapter. The dual-mode limited feedback system has two codebooks with different sizes. The proposed SER based mode selection criterion can select the better mode for current transmission.

In this chapter, the dual-mode limited feedback MISO systems are presented first. Then the proposed SER based mode selection criterion will be introduced and derived. We will show that the proposed SER based mode selection criterion also can be applied to the MISO-OFDM system. Finally, the simulation results are given.

4.1 Dual-Mode Limited Feedback Systems

The dual-mode limited feedback system is a system that has two codebooks with different sizes. Under a fixed average feedback rate, the receiver feeds back the index of the optimal beamformer from the codebook selected by the mode selection criterion. The dual-mode limited feedback system can slelect the better mode according to the current CSI and the temporal-correlation coefficient of the channel. In the high temporal-correlation channel, the dual-mode limited feedback system will select Mode I for current transmission; in the low temporal-correlation channel, the dual-mode limited feedback system will select Mode II. The dual-mode limited feedback MISO system architecture is shown in **Figure 4.1** and the mode selection scheme of the dual-mode limited feedback system is illustrated in **Figure 4.2**.
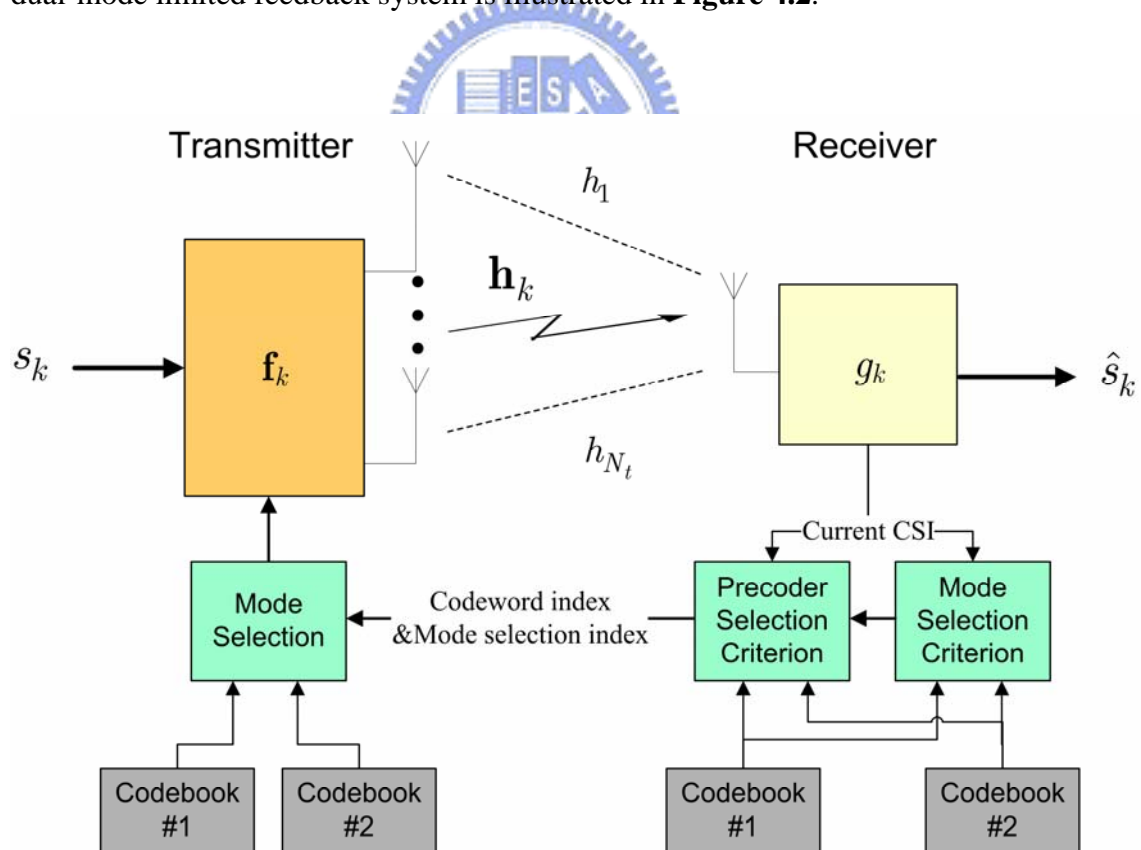
Figure 4.1: Dual-mode limited feedback system architecture
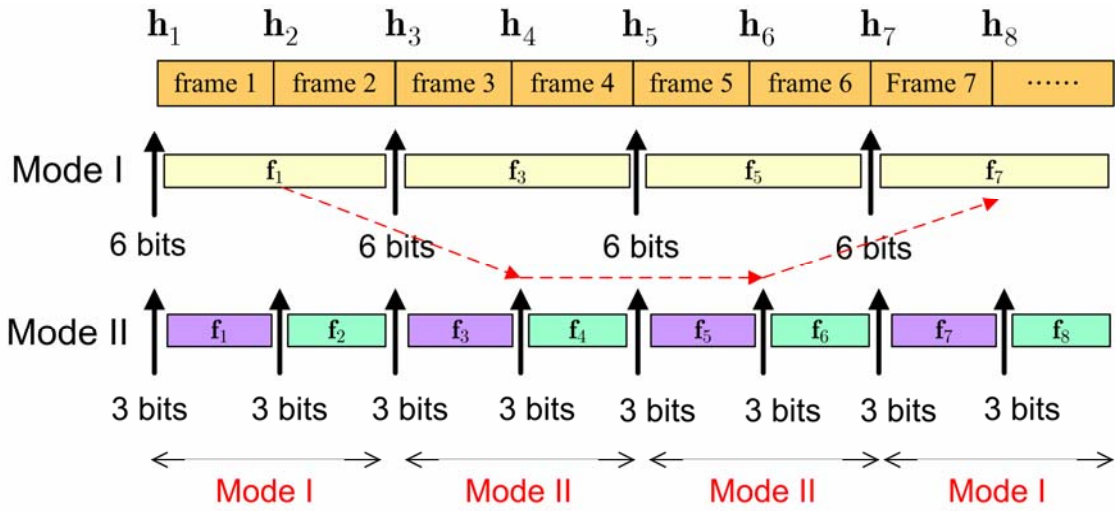
Figure 4.2: Mode selection scheme of the dual-mode limited feedback system

The receiver uses the mode selection criterion to select the better mode according to the current CSI and the temporal-correlation coefficient of the channel at the start of the k th frame. Under a fixed feedback rate at three bits per frame, if Mode I is selected, the receiver feeds back six bits at the start of the k th frame and the selected beamformer will be also used for the $(k+1)$ th frame. It feeds back **once every two frames**; if Mode II is selected, the receiver feeds back three bits at the start of the k th frame and the $(k+1)$ th frame. It feeds back **once every frame**. The dual-mode limited feedback system can switch between Mode I and Mode II by using the proposed mode selection criterion.

In the following, we will present and derive the proposed SER based mode selection criterion.

4.2 SER Based Mode Selection Criterion for MISO Systems

For selecting the better mode from Mode I and Mode II, we compare the average SER over two consecutive frames in Mode I with that in Mode II. We propose a mode selection criterion based on the average SER over two consecutive frames. The proposed SER based mode selection criterion is stated as follows:

SER Mode Selection Criterion (SER-MSC)

Select Mode I if

$$\overline{SER}_{\text{mode1}} < \overline{SER}_{\text{mode2}}, \tag{4.1}$$

where

$$\overline{SER}_{\text{mode1}} = \frac{1}{2}\left(SER_{k,\text{mode1}} + \mathbf{E}\left\{SER_{k+1,\text{mode1}}\right\}\right), \tag{4.2}$$

$$\overline{SER}_{\text{mode2}} = \frac{1}{2}\left(SER_{k,\text{mode2}} + \mathbf{E}\left\{SER_{k+1,\text{mode2}}\right\}\right). \tag{4.3}$$

$SER_{k,\text{mode1}}$ is the average SER over the k th frame in Mode I, and $SER_{k,\text{mode2}}$ is the average SER over the k th frame in Mode II. $\mathbf{E}\left\{SER_{k+1,\text{mode1}}\right\}$ is the expected value of the average SER over the $(k+1)$ th frame in Mode I and $\mathbf{E}\left\{SER_{k+1,\text{mode2}}\right\}$ is the expected value of the average SER over the $(k+1)$ th frame in Mode II.

The proposed SER based mode selection criterion will be effective if the average SER over two consecutive frames can be determined. In the following, we will derive the exact values of $SER_{k,\text{mode1}}$, $SER_{k,\text{mode2}}$, $\mathbf{E}\left\{SER_{k+1,\text{mode1}}\right\}$, and $\mathbf{E}\left\{SER_{k+1,\text{mode2}}\right\}$.

A. SER Analysis for kth Frame in Mode I
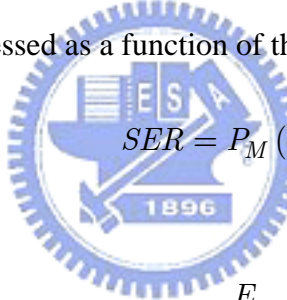
In this part, we will analyze the exact value of $SER_{k,\mathrm{mode1}}$. We take the M-QAM constellation as the example in the thesis. From [32], the symbol error rate of M-QAM constellation is

$$P_M = 1 - \left(1 - P_{\sqrt{M}}\right)^2, \tag{4.4}$$

where

$$P_{\sqrt{M}} = 2\left(1 - \frac{1}{\sqrt{M}}\right)Q\left(\sqrt{\frac{3}{M-1}\frac{E_s}{N_0}}\right), \tag{4.5}$$

and $Q(\cdot)$ is the Q-function. The symbol error rate of M-QAM constellation in Equation (4.4) can be expressed as a function of the SNR γ:

$$SER = P_M(\gamma), \tag{4.6}$$

where

$$\gamma = \frac{E_s}{N_0}. \tag{4.7}$$

From Equation (3.1), the overall power gain for the received signal is $\left|\mathbf{h}_k\mathbf{f}_k\right|^2$. The beamformer selection criterion is used to maximize this power gain $\left|\mathbf{h}_k\mathbf{f}_k\right|^2$ to minimize the SER. Thus, the beamformer selection criterion is stated as follows:

Maximum Signal-to-Noise Ratio Selection Criterion (MSNR-SC):

Pick $\mathbf{f}_{k,1}$ such that

$$\mathbf{f}_{k,1} = f(\mathbf{h}_k) = \arg\max_{\mathbf{f}_i \in \mathcal{F}_1} \left|\mathbf{h}_k\mathbf{f}_i\right|^2, \tag{4.8}$$

where $\mathbf{f}_{k,1}$ is the optimal beamformer used in Mode I for the kth frame and $\mathcal{F}_1$ is the beamformer set used in Mode I. By Equation (4.6), the average SER over the kth

frame in Mode I is

$$SER_{k,\text{mode1}} = P_M\left(\gamma_{k,\text{mode1}}\right), \tag{4.9}$$

where

$$\gamma_{k,\text{mode1}} = \left|\mathbf{h}_k\mathbf{f}_{k,1}\right|^2 \frac{E_s}{N_0}. \tag{4.10}$$

The exact value of $SER_{k,\text{mode1}}$ can be calculated by Equations (4.9) and (4.10).

B. SER Analysis for *k*th Frame in Mode II

By the same derivation of the exact value of $SER_{k,\text{mode1}}$, the average SER over the k th frame in Mode II can be written as

$$SER_{k,\text{mode2}} = P_M\left(\gamma_{k,\text{mode2}}\right), \tag{4.11}$$

where

$$\gamma_{k,\text{mode2}} = \left|\mathbf{h}_k\mathbf{f}_{k,2}\right|^2 \frac{E_s}{N_0}, \tag{4.12}$$

and

$$\mathbf{f}_{k,2} = f\left(\mathbf{h}_k\right) = \arg\max_{\mathbf{f}_i \in \mathcal{F}_2}\left|\mathbf{h}_k\mathbf{f}_i\right|^2. \tag{4.13}$$

$\mathbf{f}_{k,2}$ is the optimal beamformer used in Mode II for the k th frame, and $\mathcal{F}_2$ is the beamformer set used in Mode II. Thus, the first terms of Equation (4.2) and (4.3) can be determined by Equations (4.9) and (4.11). In the following, we will derive the expected value of $SER_{k+1,\text{mode1}}$ and $SER_{k+1,\text{mode2}}$.

C. SER Analysis for $(k+1)$th Frame in Mode I

From Equation (4.9), we know that the exact value of the average SER over the $(k+1)$th frame in Mode I, $SER_{k+1,\text{mode1}}$, can be written as

$$SER_{k+1,\text{mode1}} = P_M\left(\gamma_{k+1,\text{mode1}}\right), \tag{4.14}$$

where

$$\gamma_{k+1,\text{mode1}} = \left|\mathbf{h}_{k+1}\mathbf{f}_{k+1,1}\right|^2 \frac{E_s}{N_0}, \tag{4.15}$$

and $\mathbf{f}_{k+1,1} = \mathbf{f}_{k,1}$. It is observed that $\mathbf{f}_{k+1,1}$ is known but $\mathbf{h}_{k+1}$ is unknown at the start of the kth frame in Equation (4.15). Thus, the exact value of the average SER over the $(k+1)$th frame cannot be determined at the start of the kth frame.

Given $\mathbf{h}_k$ and $\mathbf{f}_{k+1}$, the probability density function (PDF) of the power gain over the $(k+1)$th frame $\left|\mathbf{h}_{k+1}\mathbf{f}_{k+1,1}\right|^2$ with different ρ is illustrated in **Figure 4.3**. It can be observed that the PDF of $\left|\mathbf{h}_{k+1}\mathbf{f}_{k+1,1}\right|^2$ is a function of ρ. If we can determine the PDF of $\left|\mathbf{h}_{k+1}\mathbf{f}_{k+1,1}\right|^2$ by using $\mathbf{h}_k$, $\mathbf{f}_{k+1}$, and ρ, the expected value of $SER_{k+1,\text{mode1}}$ will be determined. $SER_{k+1,\text{mode1}}$ will be substituted by $\mathbf{E}\left\{SER_{k+1,\text{mode1}}\right\}$. The average SER over two consecutive frames in Mode I is

$$\overline{SER}_{\text{mode1}} = \frac{1}{2}\left(SER_{k,\text{mode1}} + \mathbf{E}\left\{SER_{k+1,\text{mode1}}\right\}\right), \tag{4.16}$$

where $SER_{k,\text{mode1}}$ is the exact value of the average SER over the kth frame which is calculated by Equation (4.9), and $\mathbf{E}\left\{SER_{k+1,\text{mode1}}\right\}$ is the expected value of the average SER over the $(k+1)$th frame.
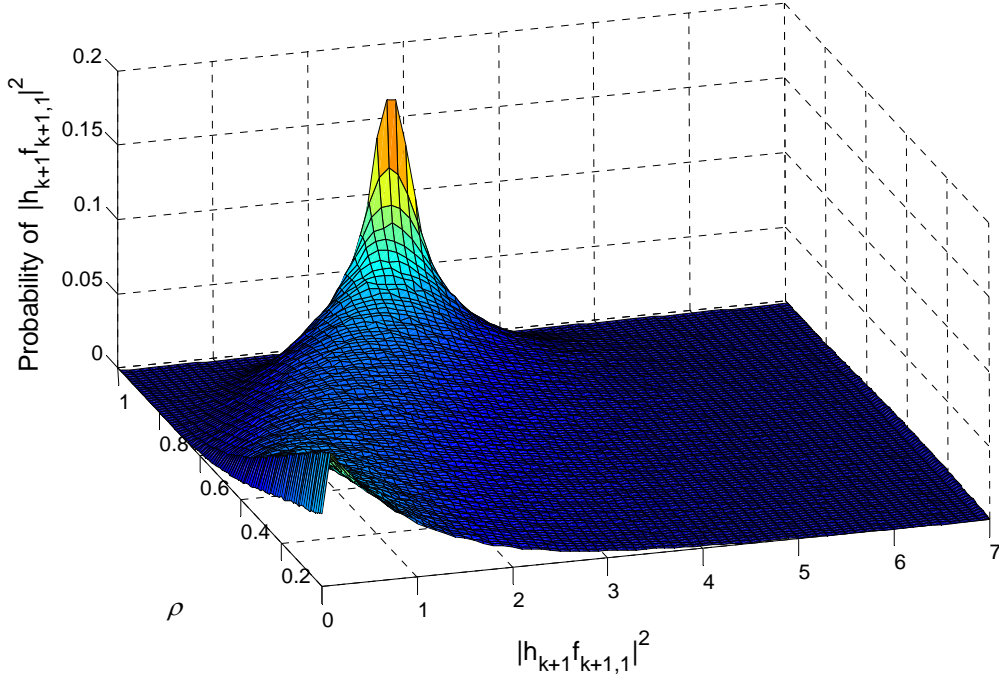
Figure 4.3: PDF of $\left|\mathbf{h}_{k+1}\mathbf{f}_{k+1,1}\right|^2$ with different ρ (given $\mathbf{h}_k$ and $\mathbf{f}_{k+1}$)

The expected value of $SER_{k+1,\text{mode1}}$ is defined as

$$\mathbf{E}\left\{SER_{k+1,\text{mode1}}\right\} = \int_0^\infty P_M\left(y\frac{E_s}{N_0}\right) \cdot f_Y\left(y \mid \mathbf{h}_k, \mathbf{f}_{k+1}, \rho\right) dy, \qquad (4.17)$$

where Y is the random variable of the received power gain $\left|\mathbf{h}_{k+1}\mathbf{f}_{k+1,1}\right|^2$. $f_Y\left(y \mid \mathbf{h}_k, \mathbf{f}_{k+1}, \rho\right)$ is the PDF of the random variable Y conditioned on a given set of $\left(\mathbf{h}_k, \mathbf{f}_{k+1}, \rho\right)$. The average SNR of the received signal over the $(k+1)$th frame in Mode I is

$$\gamma_{k+1,\text{mode1}} = \left|\mathbf{h}_{k+1}\mathbf{f}_{k+1,1}\right|^2 \frac{E_s}{N_0}. \qquad (4.18)$$

Notice that the optimal beamformer for the kth frame is also used for the $(k+1)$th frame in Mode I. That is $\mathbf{f}_{k+1,1} = \mathbf{f}_{k,1}$. It says that $\mathbf{f}_{k+1,1}$ is known in (4.18). Then we

analyze the probability distribution of the received power gain Y.

First, we define a random variable X as follows:

$$X = \mathbf{h}_{k+1}\mathbf{f}_{k+1,1} = X_r + jX_i, \tag{4.19}$$

where X_r is the real part and X_i is the imaginary part of X. From Equation (3.3), we know that $\mathbf{h}_{k+1} = \sqrt{\rho}\mathbf{h}_k + \Delta\mathbf{h}$. Thus Equation (4.19) can be rewritten as

$$X = \mathbf{h}_{k+1}\mathbf{f}_{k+1,1} = \sqrt{\rho}\mathbf{h}_k\mathbf{f}_{k+1,1} + \Delta\mathbf{h}\mathbf{f}_{k+1,1} = X_r + jX_i. \tag{4.20}$$

We define some variables to substitute $\sqrt{\rho}\mathbf{h}_k\mathbf{f}_{k+1,1}$ and $\Delta\mathbf{h}\mathbf{f}_{k+1,1}$:

$$\sqrt{\rho}\mathbf{h}_k\mathbf{f}_{k+1,1} = m_r + jm_i, \tag{4.21}$$

$$\Delta\mathbf{h}\mathbf{f}_{k+1,1} = \Delta h_r + j\Delta h_i, \tag{4.22}$$

where m_r is the real part and m_i is the imaginary part of $\sqrt{\rho}\mathbf{h}_k\mathbf{f}_{k+1,1}$. Δh_r is the real part and Δh_i is the imaginary part of $\Delta\mathbf{h}\mathbf{f}_{k+1,1}$. Equation (4.20) can be rewritten as

$$X = X_r + jX_i = (m_r + \Delta h_r) + j(m_i + \Delta h_i). \tag{4.23}$$

Because $\mathbf{f}_{k+1,1} \subset \mathcal{U}(N_t,1)$ and $\Delta\mathbf{h} \sim \mathcal{CN}\left(\mathbf{0},(1-\rho)\mathbf{I}_{N_t}\right)$ (Equation (3.2)), Δh_r and Δh_i are normally distributed random variables with zero-mean and variance $(1-\rho)/2$. Thus, X_r and X_i are normally distributed random variables with mean m_r, m_i and variances $(1-\rho)/2$:

$$X_r \sim \mathcal{N}\left(m_r, \frac{1-\rho}{2}\right), \quad X_i \sim \mathcal{N}\left(m_i, \frac{1-\rho}{2}\right). \tag{4.24}$$

The random variable Y can be rewritten as

$$Y = |X|^2 = (X_r - jX_i)(X_r + jX_i) = X_r^2 + X_i^2, \tag{4.25}$$

where

$$X_r \sim \mathcal{N}\left(m_r, \frac{1-\rho}{2}\right), \quad X_i \sim \mathcal{N}\left(m_i, \frac{1-\rho}{2}\right). \tag{4.26}$$

Equation (4.25) shows that the received power gain Y is the sum of two squared normally distributed random variables, X_r^2 and X_i^2.

Noncentral Chi-square distributed random variable is a linear combination of several normally distributed random variables [33]-[35]. The noncentral Chi-square distributed random variable Z with n degrees-of-freedom can be defined as

$$Z = \sum_{k=1}^{n}\left(\frac{X_k}{\sigma_k}\right)^2, \quad \lambda = \sum_{k=1}^{n}\left(\frac{\mu_k}{\sigma_k}\right)^2, \tag{4.27}$$

where λ is the non-centrality parameter. X_k is an independent, normally distributed random variable with mean μ_k and variance σ_k^2. The normally distributed random variables X_k are substituted by X_r and X_i and set $n = 2$ in our case. The noncentral Chi-square distributed random variable Z can be expressed as

$$Z = \frac{X_r^2}{\sigma_r^2} + \frac{X_i^2}{\sigma_i^2} = \frac{1}{(1-\rho)/2}\left(X_r^2 + X_i^2\right), \tag{4.28}$$

and

$$\lambda = \frac{m_r^2}{\sigma_r^2} + \frac{m_i^2}{\sigma_i^2} = \frac{1}{(1-\rho)/2}\left(m_r^2 + m_i^2\right) = \frac{1}{(1-\rho)/2}\left|\sqrt{\rho}\mathbf{h}_k\mathbf{f}_{k+1,1}\right|^2. \tag{4.29}$$

By Equation (4.25), Equation (4.28) can be rewritten as

$$Z = \frac{1}{(1-\rho)/2}Y. \tag{4.30}$$

Set $a = (1-\rho)/2$, we get

$$Y = aZ. \tag{4.31}$$

The probability density function of the random variable Y is

$$f_Y\left(y \mid \mathbf{h}_k, \mathbf{f}_{k+1}, \rho\right) = \frac{dF_Y\left(y \mid \mathbf{h}_k, \mathbf{f}_{k+1}, \rho\right)}{dy}$$
$$= \frac{d}{dy}\left[F_Z\left(\frac{y}{a} \mid \mathbf{h}_k, \mathbf{f}_{k+1}, \rho\right)\right] = \frac{1}{a} f_Z\left(\frac{y}{a} \mid \mathbf{h}_k, \mathbf{f}_{k+1}, \rho\right),$$

(4.32)

where $f_Z(z)$ is the PDF of the noncentral Chi-square distributed random variable with $\lambda = \frac{1}{a}\left|\sqrt{\rho}\mathbf{h}_k\mathbf{f}_{k+1,1}\right|^2$ and two degrees-of-freedom. $f_Z(z)$ is defined as follows [35]:

$$f_Z(z; n, \lambda) = \frac{1}{2} e^{-(z+\lambda)/2}\left(\frac{z}{\lambda}\right)^{(n-2)/4} I_{(n-2)/2}\left(\sqrt{\lambda z}\right), \quad z > 0, \quad (4.33)$$

where $I_m(x)$ is a modified Bessel function of the first kind of order m which is given by

$$I_m(x) = \left(\frac{x}{2}\right)^m \sum_{j=1}^{\infty} \frac{\left(x^2/4\right)^j}{j!\,\Gamma(m+j+1)}. \quad (4.34)$$

Thus, the expected value of $SER_{k+1,\text{mode1}}$ is

$$\mathbf{E}\left\{SER_{k+1,\text{mode1}}\right\} = \int_0^{\infty} P_M\left(y\frac{E_s}{N_0}\right) \cdot f_Y\left(y \mid \mathbf{h}_k, \mathbf{f}_{k+1}, \rho\right) dy$$
$$= \int_0^{\infty} P_M\left(y\frac{E_s}{N_0}\right) \cdot \frac{1}{a} f_Z\left(\frac{y}{a} \mid \mathbf{h}_k, \mathbf{f}_{k+1}, \rho\right) dy,$$

(4.35)

where $f_Z(z)$ is the PDF of the noncentral Chi-square distribution with $\lambda = \frac{1}{a}\left|\sqrt{\rho}\mathbf{h}_k\mathbf{f}_{k+1,1}\right|^2$ and two degrees-of-freedom. We can calculate $\mathbf{E}\left\{SER_{k+1,\text{mode1}}\right\}$ by the above derivation. Thus the average SER over two consecutive frames for Mode I can be determined.

D. SER Analysis for $(k+1)$th Frame in Mode II

The difference between the SER analysis of the $(k + 1)$th frame for Mode I and that for Mode II is the beamformer for the $(k + 1)$th frame. In Mode I, the beamformer for the $(k + 1)$th frame is known at the start of the the kth frame; in Mode II, the beamformer for the $(k + 1)$th frame is unknown at the start of the the kth frame because it will be reselected at the start of the $(k + 1)$th frame. The receiver does not know which beamformer will be selected. In this part, we will follow the analysis methods in [12] and calculate the expected value of $SER_{k+1,\text{mode2}}$.

Define a normalized channel vector as

$$\tilde{\mathbf{h}}_{k+1} = \frac{\mathbf{h}_{k+1}}{\left\|\mathbf{h}_{k+1}\right\|}, \tag{4.36}$$

such that $\mathbf{h}_{k+1} = \left\|\mathbf{h}_{k+1}\right\| \cdot \tilde{\mathbf{h}}_{k+1}$ and $\left\|\tilde{\mathbf{h}}_{k+1}\right\| = 1$. Then we decompose the average SNR of the received signal over the $(k + 1)$th frame in Mode II:

$$
\begin{aligned}
\gamma_{k+1,\text{mode2}} &= \left\|\mathbf{h}_{k+1}\right\|^2 \frac{E_s}{N_0} \max_{\mathbf{f}_i \in \mathcal{F}_2} \left| \frac{\mathbf{h}_{k+1}}{\left\|\mathbf{h}_{k+1}\right\|} \mathbf{f}_i \right|^2 \\
&= \left\|\mathbf{h}_{k+1}\right\|^2 \frac{E_s}{N_0} \max_{\mathbf{f}_i \in \mathcal{F}_2} \left| \tilde{\mathbf{h}}_{k+1} \mathbf{f}_i \right|^2 \\
&= \left\|\mathbf{h}_{k+1}\right\|^2 \frac{E_s}{N_0} \left[1 - \min_{\mathbf{f}_i \in \mathcal{F}_2} d^2 \left(\tilde{\mathbf{h}}_{k+1}^H, \mathbf{f}_i \right) \right],
\end{aligned} \tag{4.37}
$$

where $\mathbf{f}_i \in \mathcal{F}_2$ and $d(\cdot)$ is the chordal distance which is defined as $d(\mathbf{w}_i, \mathbf{w}_j) = \sqrt{1 - \left| \mathbf{w}_i^H \mathbf{w}_j \right|^2}$. To simplify the notation, we define the average transmit SNR $\bar{\gamma} = E_s / N_0$ and two random variables:

$$\gamma_h = \left\|\mathbf{h}_{k+1}\right\|^2, \tag{4.38}$$

$$U = \min_i d^2 \left(\tilde{\mathbf{h}}_{k+1}^H, \mathbf{f}_i \right). \tag{4.39}$$

Equation (4.37) can be rewritten as

$$\gamma_{k+1,\text{mode2}} = \gamma_h \left(1 - U\right) \overline{\gamma}, \tag{4.40}$$

where U is a random variable within the interval $[0,1]$, i.e., $U \in [0,1]$. The expected value of $SER_{k+1,\text{mode2}}$ can be expressed as

$$\mathbf{E}\left\{SER_{k+1,\text{mode2}}\right\} = \int\limits_{\gamma_h=0}^{\infty} \int\limits_{u=0}^{1} P_M\left(\gamma_h\left(1-u\right)\overline{\gamma}\right) f_{\gamma_h}(\gamma_h \mid \mathbf{h}_k, \rho) f_U(u) d\gamma_h du \tag{4.41}$$

$$= \int\limits_{\gamma_h=0}^{\infty} \int\limits_{u=0}^{1} P_M\left(\gamma_h\left(1-u\right)\overline{\gamma}\right) f_{\gamma_h}(\gamma_h \mid \mathbf{h}_k, \rho) dF_U(u) d\gamma_h, \tag{4.42}$$

where $P_M(\cdot)$ is the SER of M-QAM constellation defined in Equation (4.6) and $F_U(u)$ is the cumulative distribution function (CDF) of U.

Notice that $F_U(u)$ depends on the particular beamformer design $\mathcal{F}_2$. To obtain the exact SER in Equation (4.41), we have to find the exact $F_U(u)$ for each particular beamformer and the exact $f_{\gamma_h}(\gamma_h)$. Unfortunately, the exact $F_U(u)$ is difficult to obtain. To solve this problem, we use a lower bound on the outage probability derived in [12] to substitute the exact $F_U(u)$ and then derive the exact $f_{\gamma_h}(\gamma_h)$ in the following.

(a) Upper Bound of $F_U(u)$

The work in [12] shows that the upper bound of $F_U(u)$ is defined as

$$F_U(u) \leq \tilde{F}_U(u) = \begin{cases} Nu^{N_t-1}, & 0 \leq u < \left(\dfrac{1}{N}\right)^{\frac{1}{N_t-1}} \\ 1, & u \geq \left(\dfrac{1}{N}\right)^{\frac{1}{N_t-1}} \end{cases}, \tag{4.43}$$

where N is the codebook size and N_t is the number of transmit antennas. The function $\tilde{F}_U(u)$ is derived under the geometrical framework presented in [36]. The

proof of $F_U(u) \le \tilde{F}_U(u)$ is given in [12]. We use $\tilde{F}_U(u)$ derived in [12] to substitute $F_U(u)$ in Equation (4.42).

(b) Exact $f_{\gamma_h}(\gamma_h)$

From Equation (4.38), γ_h is defined as

$$
\begin{aligned}
\gamma_h &= \left\| \mathbf{h}_{k+1} \right\|^2 = \left\langle \mathbf{h}_{k+1}, \mathbf{h}_{k+1} \right\rangle \\
&= \left(\left(X_{1,r}^{k+1} \right)^2 + \left(X_{1,i}^{k+1} \right)^2 \right) + \ldots + \left(\left(X_{N_t,r}^{k+1} \right)^2 + \left(X_{N_t,i}^{k+1} \right)^2 \right),
\end{aligned}
\tag{4.44}
$$

where $\left\langle \mathbf{u}, \mathbf{v} \right\rangle = \mathbf{u}^H \mathbf{v}$ is the complex inner product of vectors $\mathbf{u}$ and $\mathbf{v}$. $X_{j,r}^{k+1}$ is the real part and $X_{j,i}^{k+1}$ is the imaginary part of the jth element of the channel vector $\mathbf{h}_{k+1} = \left[h_1^{k+1}, h_2^{k+1}, \ldots, h_{N_t}^{k+1} \right]$. By the same results derived from Equations (4.19) to (4.26), it is observed that the random variable γ_h is a linear combination of $N_t \times 2$ normally distributed random variables. The distributions of $X_{j,r}^{k+1}$ and $X_{j,i}^{k+1}$ are

$$
X_{j,r}^{k+1} \sim \mathcal{N}\left(m_{j,r}^{k+1}, \frac{1-\rho}{2} \right), \quad X_{j,i}^{k+1} \sim \mathcal{N}\left(m_{j,i}^{k+1}, \frac{1-\rho}{2} \right),
\tag{4.45}
$$

where j is the index of transmit antennas, $m_{j,r}^{k+1}$ is the real part and $m_{j,i}^{k+1}$ is the imaginary part of $\sqrt{\rho} h_j^k$ under a condition that $\mathbf{h}_k = \left[h_1^k, \ldots, h_{N_t}^k \right]$ is given. From [33], γ_h is a noncentral Chi-square distributed random variable with $N_t \times 2$ degrees-of-freedom, $\lambda = \frac{1}{a} \left\| \sqrt{\rho} \mathbf{h}_k \right\|^2$, and $a = \frac{1-\rho}{2}$. By the same results derived from Equations (4.27) to (4.31), the random variable γ_h can be written as

$$
\gamma_h = aZ,
\tag{4.46}
$$

where Z is a noncentral Chi-square distributed random variable with $N_t \times 2$ degrees-of-freedom, $\lambda = \frac{1}{a} \left\| \sqrt{\rho} \mathbf{h}_k \right\|^2$, and $a = \frac{1-\rho}{2}$. The probability density function of the random variable γ_h can be written as

$$f_{\gamma_h}\left(\gamma_h \mid \mathbf{h}_k, \rho\right) = \frac{dF_{\gamma_h}\left(\gamma_h \mid \mathbf{h}_k, \rho\right)}{d\gamma_h}$$

$$= \frac{d}{d\gamma_h}\left[F_Z\left(\frac{\gamma_h}{a} \mid \mathbf{h}_k, \rho\right)\right] = \frac{1}{a}f_Z\left(\frac{\gamma_h}{a} \mid \mathbf{h}_k, \rho\right), \tag{4.47}$$

where $f_Z(z)$ is the PDF of the noncentral Chi-square distributed random variable with $N_t \times 2$ degrees-of-freedom and $\lambda = \frac{1}{a}\left\|\sqrt{\rho}\mathbf{h}_k\right\|^2$, and it is defined in Equation (4.33).

We have determined the upper bound of $F_U(u)$ and the exact $f_{\gamma_h}(\gamma_h)$. The expected value of $SER_{k+1,\text{mode2}}$ will be substituted by **the lower bound** of the expected value of $SER_{k+1,\text{mode2}}$. The lower bound of the expected value of $SER_{k+1,\text{mode2}}$ is

$$\mathbf{E}\left\{SER_{k+1,\text{mode2}}\right\}_{\text{lb}}$$

$$= \int_{r_h=0}^{\infty} \int_{u=0}^{\left(\frac{1}{N}\right)^{\frac{1}{N_t-1}}} P_M\left(\gamma_h\left(1-u\right)\overline{\gamma}\right)\frac{1}{a}f_Z\left(\frac{\gamma_h}{a} \mid \mathbf{h}_k, \rho\right)\left(N_t - 1\right)Nu^{N_t-2}d\gamma_h du, \tag{4.48}$$

where Z is a noncentral Chi-square distributed random variable with $N_t \times 2$ degrees-of-freedom, $\lambda = \frac{1}{a}\left\|\sqrt{\rho}\mathbf{h}_k\right\|^2$, and $a = \frac{1-\rho}{2}$.

By Equations (4.9), (4.11), (4.35), and (4.48), all terms of the proposed mode selection criterion are determined. Notice that $\mathbf{E}\left\{SER_{k+1,\text{mode2}}\right\}$ is substituted by $\mathbf{E}\left\{SER_{k+1,\text{mode2}}\right\}_{\text{lb}}$. The proposed SER based mode selection criterion is stated as follows:

SER Mode Selection Criterion (SER-MSC)

Select Mode I if

$$\overline{SER}_{\text{mode1}} < \overline{SER}_{\text{mode2}}, \tag{4.49}$$

where

$$\overline{SER}_{\text{mode1}} = \frac{1}{2}\Big(SER_{k,\text{mode1}} + \mathbf{E}\big\{SER_{k+1,\text{mode1}}\big\}\Big), \qquad (4.50)$$

$$\overline{SER}_{\text{mode2}} = \frac{1}{2}\Big(SER_{k,\text{mode2}} + \mathbf{E}\big\{SER_{k+1,\text{mode2}}\big\}_{\text{lb}}\Big). \qquad (4.51)$$

$SER_{k,\text{mode1}}$ is the average SER over the k th frame in Mode I, and $SER_{k,\text{mode2}}$ is

the average SER over the k th frame in Mode II. $\mathbf{E}\big\{SER_{k+1,\text{mode1}}\big\}$ is the expected

value of the average SER over the $(k+1)$ th frame in Mode I, and

$\mathbf{E}\big\{SER_{k+1,\text{mode2}}\big\}_{\text{lb}}$ is the lower bound of the expected value of the average SER over

the $(k+1)$ th frame in Mode II.

From the above derivation, we can use the proposed mode selection criterion to select the better mode at the start of the k th frame for current transmission in a MISO system.

4.3 SER Based Mode Selection Criterion for MISO-OFDM Systems

In this section, we will introduce the OFDM system first. Then we will show that the proposed SER based mode selection criterion can be readily applied to MISO-OFDM systems.
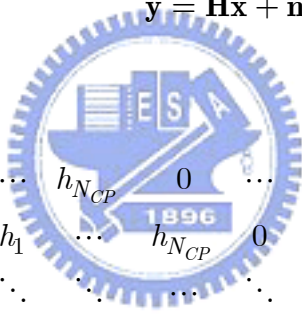
4.3.1 Review of OFDM

OFDM is chosen over a single carrier solution due to its lower complexity of equalizers for high delay spread channels or high data rates. A broadband signal is broken down into multiple narrowband carriers (tones), where each carrier is more robust to multipath. In order to maintain orthogonality amongst tones, a cyclic prefix (CP) is added which has a length greater than the expected delay spread. With proper coding and interleaving across frequencies, multipath turns into an OFDM system

advantage by yielding frequency diversity.

OFDM can be implemented efficiently by using fast Fourier transform (FFT) at the transmitter and receiver. At the receiver, FFT reduces the channel response into a multiplicative constant on a tone-by-tone basis. With MIMO, the channel response becomes a matrix. Since each tone can be equalized independently, the complexity of space-time equalizers is avoided. Multipath remains an advantage for a MIMO-OFDM system since frequency selectivity caused by multipath improves the rank distribution of the channel matrices across frequency tones, thereby increasing capacity.

Assuming that the channel length is smaller than N_{CP} (number of samples in CP), we can express the received signal vector $\mathbf{y}$ as

$$\mathbf{y} = \mathbf{H}\mathbf{x} + \mathbf{n} \tag{4.52}$$

$$\underbrace{\begin{bmatrix} y_{N_{FFT}-1} \\ \vdots \\ y_0 \end{bmatrix}}_{\mathbf{y}} = \underbrace{\begin{bmatrix} h_0 & h_1 & \cdots & h_{N_{CP}} & 0 & \cdots & 0 \\ 0 & h_0 & h_1 & \cdots & h_{N_{CP}} & 0 & \vdots \\ 0 & 0 & \ddots & \ddots & \cdots & \ddots & 0 \\ 0 & \cdots & 0 & h_0 & h_1 & \cdots & h_{N_{CP}} \end{bmatrix}}_{\mathbf{H}} \underbrace{\begin{bmatrix} x_{N_{FFT}-1} \\ \vdots \\ x_0 \\ x_{-1} \\ \vdots \\ x_{-N_{CP}} \end{bmatrix}}_{\mathbf{x}} + \underbrace{\begin{bmatrix} n_{N_{FFT}-1} \\ \vdots \\ n_0 \end{bmatrix}}_{\mathbf{n}},$$

$$\tag{4.53}$$

where $\mathbf{x}$ is the transmit signal vector and $\mathbf{n}$ is the noise vector. N_{FFT} is the FFT length. When we perform the singular value decomposition (SVD), we have

$$\mathbf{H} = \mathbf{V}_L \mathbf{\Lambda} \mathbf{V}_R^H, \tag{4.54}$$

where $\mathbf{V}_L \mathbf{V}_L^H = \mathbf{I}$ and $\mathbf{V}_R \mathbf{V}_R^H = \mathbf{I}$. If we let $\mathbf{x} = \mathbf{V}_R \mathbf{X}$ and $\mathbf{Y} = \mathbf{V}_L^H \mathbf{y}$, then we can get

$$\mathbf{Y} = \mathbf{V}_L^H \mathbf{y} = \mathbf{V}_L^H (\mathbf{Hx} + \mathbf{n}) = \mathbf{V}_L^H \mathbf{H} \mathbf{V}_R \mathbf{X} + \underbrace{\mathbf{N}}_{\mathbf{V}_L^H \mathbf{n}} = \mathbf{\Lambda X} + \mathbf{N}. \qquad (4.55)$$

It is interesting to note that when the guard period contains a CP, that is, $x_{-i} = x_{N-i}$ for $i = 1, ..., N_{CP}$, Equation (4.53) can be rewritten in a more compact matrix form

$$\begin{bmatrix} y_{N_{FFT}-1} \\ \vdots \\ y_0 \end{bmatrix} = \begin{bmatrix} h_0 & h_1 & \cdots & h_{N_{CP}} & 0 & \cdots & 0 \\ 0 & h_0 & h_1 & \cdots & h_{N_{CP}} & \ddots & 0 \\ \vdots & \ddots & \ddots & \ddots & \ddots & \ddots & \vdots \\ 0 & \cdots & 0 & h_0 & h_1 & \cdots & h_{N_{CP}} \\ h_{N_{CP}} & 0 & \cdots & 0 & h_0 & \cdots & h_{N_{CP}-1} \\ \vdots & \ddots & \ddots & \ddots & \ddots & \ddots & \vdots \\ h_1 & \cdots & h_{N_{CP}} & 0 & \cdots & 0 & h_0 \end{bmatrix} \begin{bmatrix} x_{N_{FFT}-1} \\ \vdots \\ x_0 \end{bmatrix} + \begin{bmatrix} n_{N_{FFt}-1} \\ \vdots \\ n_0 \end{bmatrix},$$

$$(4.56)$$

and $\mathbf{H}$ becomes the so called "circulant matrix" and has the property $\mathbf{H} = \mathbf{F}^H \mathbf{\Lambda F}$, where $\mathbf{F}$ is a discrete Fourier transform (DFT) matrix with klth entry as

$$\mathbf{F}_{kl} = \frac{1}{\sqrt{N_{FFT}}} e^{-j2\pi \frac{kl}{N_{FFT}}}, \qquad (4.57)$$

and the transformed symbol is $\mathbf{x} = \mathbf{F}^H \mathbf{X}$ (inverse DFT (IDFT) of $\mathbf{x}$). Thus $\mathbf{X}$ can be interpreted as the symbols in the frequency domain. At the receiver, we have the received signal $\mathbf{y}$ being transformed to $\mathbf{Y}$

$$\mathbf{Y} = \mathbf{Fy} = \mathbf{F}(\mathbf{Hx} + \mathbf{n}) = \underbrace{\mathbf{FHF}^H}_{\mathbf{\Lambda}} \mathbf{X} + \underbrace{\mathbf{F}^H \mathbf{n}}_{\mathbf{N}} = \mathbf{\Lambda X} + \mathbf{N}. \qquad (4.58)$$

Now, we can realize that by using CP, the OFDM modulation is equivalent to multiplying the frequency domain signals of the OFDM symbol (that is, $\mathbf{X}$) with the channel frequency response $\mathbf{\Lambda}$ which is a diagonal matrix.

4.3.2 Multipath First-Order Markov MISO Channel Model

In this section, we will show that the multipath first-order Markov MISO channel model has the same property with the first-order Markov MISO channel model which is assumed and introduced in Chapter 3. Thus, the proposed SER based mode selection criterion can be applied to MISO-OFDM systems.

Consider a multipath MISO channel with channel order L_{ch} and temporal-correlation coefficient ρ. The time-varying property of the multipath MISO channel can be characterized by the first-order Markov channel model (Equation (3.3)). The first-order Markov channel model is only characterized by the one-tap temporal-correlation coefficient ρ. From Equation (4.56), the channel matrix between the jth transmit antenna and the receive antenna for the $(k+1)$th OFDM symbol time can be written as

$$\mathbf{H}_j^{k+1} = \sqrt{\rho}\mathbf{H}_j^k + \Delta\mathbf{H}_j, \tag{4.59}$$

where

$$\mathbf{H}_j^{k+1} = \begin{bmatrix} h_{j,0}^{k+1} & h_{j,1}^{k+1} & \cdots & h_{j,N_{CP}}^{k+1} & 0 & \cdots & 0 \\ 0 & h_{j,0}^{k+1} & h_{j,1}^{k+1} & \cdots & h_{j,N_{CP}}^{k+1} & \ddots & 0 \\ \vdots & \ddots & \ddots & \ddots & \ddots & \ddots & \vdots \\ 0 & \cdots & 0 & h_{j,0}^{k+1} & h_{j,1}^{k+1} & \cdots & h_{j,N_{CP}}^{k+1} \\ h_{j,N_{CP}}^{k+1} & 0 & \cdots & 0 & h_{j,0}^{k+1} & \cdots & h_{j,N_{CP}-1}^{k+1} \\ \vdots & \ddots & \ddots & \ddots & \ddots & \ddots & \vdots \\ h_{j,1}^{k+1} & \cdots & h_{j,N_{CP}}^{k+1} & 0 & \cdots & 0 & h_{j,0}^{k+1} \end{bmatrix}, \tag{4.60}$$

$$\mathbf{H}_j^k = \begin{bmatrix} h_{j,0}^k & h_{j,1}^k & \cdots & h_{j,N_{CP}}^k & 0 & \cdots & 0 \\ 0 & h_{j,0}^k & h_{j,1}^k & \cdots & h_{j,N_{CP}}^k & \ddots & 0 \\ \vdots & \ddots & \ddots & \ddots & \ddots & \ddots & \vdots \\ 0 & \cdots & 0 & h_{j,0}^k & h_{j,1}^k & \cdots & h_{j,N_{CP}}^k \\ h_{j,N_{CP}}^k & 0 & \cdots & 0 & h_{j,0}^k & \cdots & h_{j,N_{CP}-1}^k \\ \vdots & \ddots & \ddots & \ddots & \ddots & \ddots & \vdots \\ h_{j,1}^k & \cdots & h_{j,N_{CP}}^k & 0 & \cdots & 0 & h_{j,0}^k \end{bmatrix}, \quad (4.61)$$

and

$$\Delta\mathbf{H}_j = \begin{bmatrix} \Delta h_{j,0} & \Delta h_{j,1} & \cdots & \Delta h_{j,N_{CP}} & 0 & \cdots & 0 \\ 0 & \Delta h_{j,0} & \Delta h_{j,1} & \cdots & \Delta h_{j,N_{CP}} & \ddots & 0 \\ \vdots & \ddots & \ddots & \ddots & \ddots & \ddots & \vdots \\ 0 & \cdots & 0 & \Delta h_{j,0} & \Delta h_{j,1} & \cdots & \Delta h_{j,N_{CP}} \\ \Delta h_{j,N_{CP}} & 0 & \cdots & 0 & \Delta h_{j,0} & \cdots & \Delta h_{j,N_{CP}-1} \\ \vdots & \ddots & \ddots & \ddots & \ddots & \ddots & \vdots \\ \Delta h_{j,1} & \cdots & \Delta h_{j,N_{CP}} & 0 & \cdots & 0 & \Delta h_{j,0} \end{bmatrix}.$$

$$(4.62)$$

$h_{j,n}^{k+1}$ is the channel coefficient of the n th tap between the j th transmit antenna and the receive antenna for the $(k+1)$ th OFDM symbol time. $h_{j,n}^k$ is the channel coefficient of the n th tap between the j th transmit antenna and the receive antenna for the k th OFDM symbol time. We assume that the path loss vector is $\left[P_{\text{loss},0},...,P_{\text{loss},N_{CP}} \right]$, $\sum_{n=0}^{N_{CP}} P_{\text{loss},n} = 1$, and $\mathbf{E}\left\{ \left\| h_{j,0}^{k+1},...,h_{j,N_{CP}}^{k+1} \right\|^2 \right\} = 1$ for convenience. $\Delta h_{j,n}$ is a complex normally distributed random variable of the n th tap between the j th transmit antenna and the receive antenna with zero-mean and variance $(1-\rho) \cdot P_{\text{loss},n}$. ρ is the temporal-correlation coefficient ($0 \le \rho \le 1$). A small $\rho(=0)$ implies the fast fading environment and a large $\rho(=1)$ corresponds to the time-invariant channel. We also assume that the channel length is smaller than

N_{CP}, that is $L_{ch} + 1 < N_{CP}$.

From Equation (4.58), the channel frequency response of $\mathbf{H}_j^{k+1}$ can be written as

$$\mathbf{F}\mathbf{H}_j^{k+1}\mathbf{F}^H = \sqrt{\rho}\mathbf{F}\mathbf{H}_j^k\mathbf{F}^H + \mathbf{F}\Delta\mathbf{H}_j\mathbf{F}^H. \tag{4.63}$$

Equation (4.63) can be rewritten as

$$\mathbf{\Lambda}_j^{k+1} = \sqrt{\rho}\mathbf{\Lambda}_j^k + \Delta\mathbf{\Lambda}_j, \tag{4.64}$$

where $\mathbf{\Lambda}_j^{k+1}$ is the channel frequency response between the jth transmit antenna and the receive antenna for the $(k+1)$th OFDM symbol time, and $\mathbf{\Lambda}_j^k$ is the channel frequency response between the jth transmit antenna and the receive antenna for the kth OFDM symbol time. $\Delta\mathbf{\Lambda}_j$ is the innovation matrix between the jth transmit antenna and the receive antenna. $\mathbf{\Lambda}_j^{k+1}$, $\mathbf{\Lambda}_j^k$, and $\Delta\mathbf{\Lambda}_j$ are all diagonal matrices.

We assume that $\Delta h_{j,n}$ is a complex normally distributed random variable with zero-mean and variance $(1-\rho)P_{\mathrm{loss},n}$ and $\sum_{n=0}^{N_{CP}} P_{\mathrm{loss},n} = 1$. Under this condition, the total variance of $\Delta\mathbf{H}_j$ is $(1-\rho)\cdot N_{FFT}$. Because DFT is a linear transformation and $\mathbf{F}\mathbf{F}^H = \mathbf{I}$, the total variance of the diagonal matrix $\Delta\mathbf{\Lambda}_j = \mathbf{F}\Delta\mathbf{H}_j\mathbf{F}^H$ is also $(1-\rho)\cdot N_{FFT}$ and each element of the diagonal matrix $\Delta\mathbf{\Lambda}_j$ is a complex normally distributed random variable with zero-mean and variance $(1-\rho)$. All elements are mutually dependent normal random variables with zero-mean and variance $(1-\rho)$. Equation (4.64) can be rewritten as

$$\Lambda_{j,nn}^{k+1} = \sqrt{\rho}\Lambda_{j,nn}^k + \Delta\Lambda_{j,nn}, \qquad \text{for} \quad n = 1,...,N_{FFT}, \tag{4.65}$$

where $\Lambda_{j,nn}^{k+1}$ is the channel frequency response of the nth subcarrier between the

jth transmit antenna and the receive antenna for the $(k+1)$th OFDM symbol time,

and $\Lambda_{j,nn}^{k}$ is the channel frequency response of the nth subcarrier between the jth

transmit antenna and the receive antenna for the kth OFDM symbol time. $\Delta\Lambda_{j,nn}$ is

a complex normally distributed random variable with zero-mean and variance $(1-\rho)$.

Consider a MISO-OFDM system with N_t transmit antenna and one receive

antenna. For the nth subcarrier, we can collect $\Lambda_{j,nn}^{k+1}$, for $j=1,...,N_t$, as a row

vector $\boldsymbol{\Lambda}_{ch,n}^{k+1} = \left[\Lambda_{1,nn}^{k+1},...,\Lambda_{N_t,nn}^{k+1}\right]$. The MISO channel frequency response of the nth

subcarrier for the $(k+1)$th OFDM symbol time can be written as

$$\boldsymbol{\Lambda}_{ch,n}^{k+1} = \sqrt{\rho}\boldsymbol{\Lambda}_{ch,n}^{k} + \Delta\boldsymbol{\Lambda}_{ch,n}, \qquad \text{for} \quad n=1,...,N_{FFT}, \qquad (4.66)$$

where $\Delta\boldsymbol{\Lambda}_{ch,n} \sim \mathcal{CN}\left(\mathbf{0},(1-\rho)\mathbf{I}_{N_t}\right)$. All elements of $\Delta\boldsymbol{\Lambda}_{ch,n}$ are independent

because of the independence between N_t transmit antennas.

Comparing Equation (4.66) with Equation (3.3), we see that the frequency

response of the multipath first-order Markov MISO channel model has the same

time-varying property with the first-order Markov MISO channel model defined in

Equation (3.3). Thus the proposed SER based mode selection criterion can be used to

select the better mode tone by tone in the MISO-OFDM system.

4.4 Computer Simulations

In the following, we will illustrate the performances of the single-mode and dual-mode limited feedback MISO systems. We also consider a MISO-OFDM system in the simulations and illustrate the performances of the single-mode and the dual-mode limited feedback MISO-OFDM systems. The schemes of Mode I and Mode II for single-carrier systems and multi-carrier systems are commented in **Table 3.4**

(a) Dual-mode limited feedback MISO system

We consider a dual-mode limited feedback system in this simulation. **Table 4.1** lists all parameters used in our simulation. This simulation uses 16-QAM modulation and one data substream on a 4×1 wireless system. The transmit beamforming codebooks in IEEE 802.16-2005 are applied in the simulation. The average feedback rate is fixed at three bits per frame. The dual-mode system uses the proposed SER based mode selection criterion to select the better mode for current transmission. Each frame consists of 128 symbols and each transmission consists of 16 frames.

The channel is assumed to be quasi-static and Rayleigh fading. The channel gains of two consecutive frames also follow the first-order Markov channel model (3.3). The elements of the random perturbation $\Delta \mathbf{h}$ in Equation (3.3) are assumed to be i.i.d. zero-mean complex Gaussian with variance $(1 - \rho)$. SNR is defined as the ratio of the average received signal power to the average received noise power. Perfect channel knowledge known at the receiver and the error-free feedback channel are also assumed in the simulation. SER performances of the single-mode systems (operating in Mode I and Mode II) and the dual-mode system with the SER based mode selection criterion are shown in Figures 4.4-4.7 with $\rho = 1, 0.9, 0.8, 0.7$.

Table 4.1: Simulation environment of the dual-mode limited feedback MISO system

| Parameter	Values
Channel	Rayleigh fading channel (First-order Markov channel model)
Modulation	16-QAM
Number of transmit antenna	4
Number of receive antenna	1
Fixed average feedback rate	3 bits per frame
Frame length	128 symbols
Number of frames	16 frames per transmission
Codebook	Transmit beamforming codebooks in IEEE 802.16-2005

When $\rho = 1$, **Figure 4.4** illustrates the SER performances of the dual-mode system and the single-mode system. The performance of the dual-mode system is close to that of Mode I (6-bit beamformer) and better than that of Mode II (3-bit beamformer). It is observed that the dual-mode system mainly selects Mode I for current transmission but not Mode II.

When $\rho = 0.9$, **Figure 4.5** illustrates that the SER performance of the dual-mode system still is better than that of the single-mode system. The curve of Mode II crosses the curve of Mode I at SNR=14 dB. The single-mode system operating in Mode I losses some diversity gain, but the dual-mode does not. At SNR=14 dB, the dual-mode system can switch between Mode I and Mode II, so it has better performance than the single-mode system operating either in Mode I or Mode II.

When $\rho = 0.8$, **Figure 4.6** shows that the SER performance of Mode I becomes poorer than that of Mode I in **Figure 4.5**. The curve Mode II crosses the curve of Mode I at SNR=10 dB. The dual-mode system with SER-MSC is more robust than the

single-mode system. At low SNR region, the dual-mode system mainly selects Mode I for transmission. At SNR=10 dB, the dual-mode system can switch between Mode I and Mode II, so it has better performance than the single-mode systems. At high SNR region, the performance of the dual-mode system is close to that of Mode II. It states that the dual-mode system mainly selects Mode II at high SNR region.

When $\rho = 0.7$, **Figure 4.7** shows that the performance of the dual-mode system is still better than that of the single-mode systems. At low SNR region, the dual-mode system mainly selects Mode I because the performance of Mode I is better than that of Mode II. At high SNR region, the dual-mode system mainly selects Mode II because the performance of Mode II is better than that of Mode I. It states that the dual-mode system is more robust than the single-mode system in the time-varying channel.
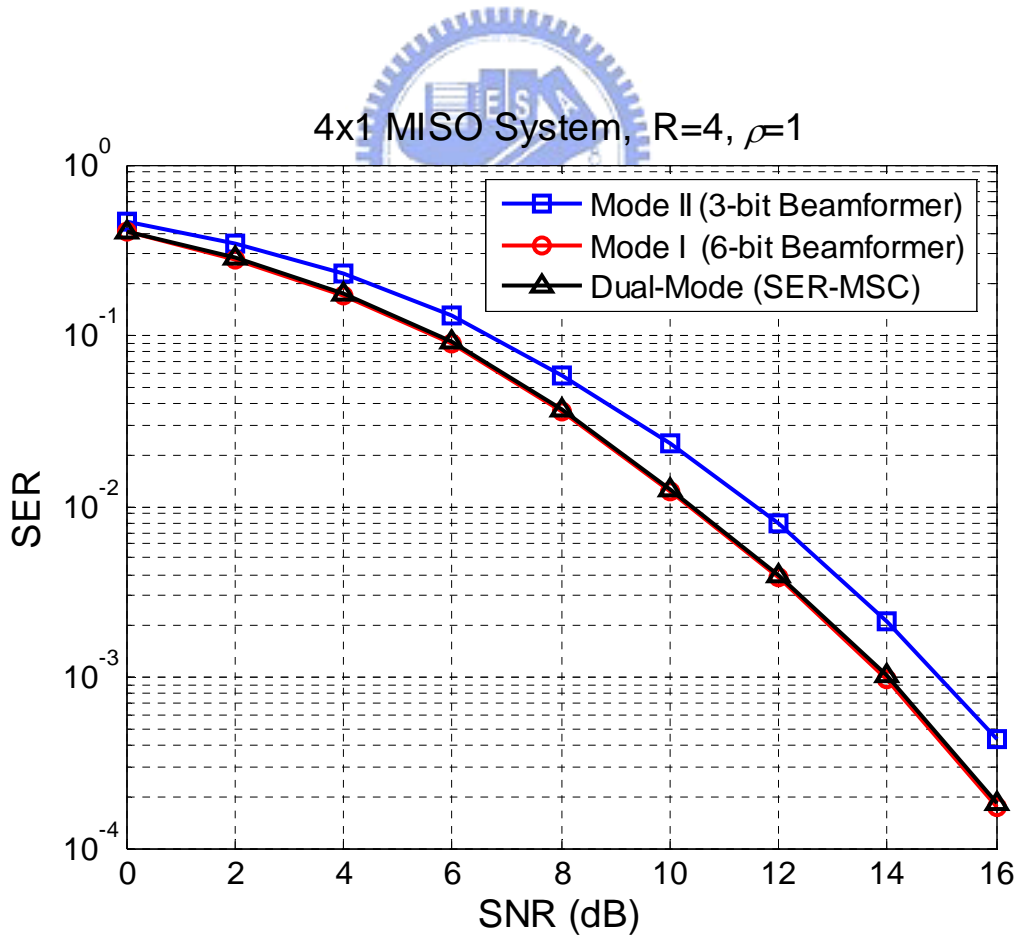
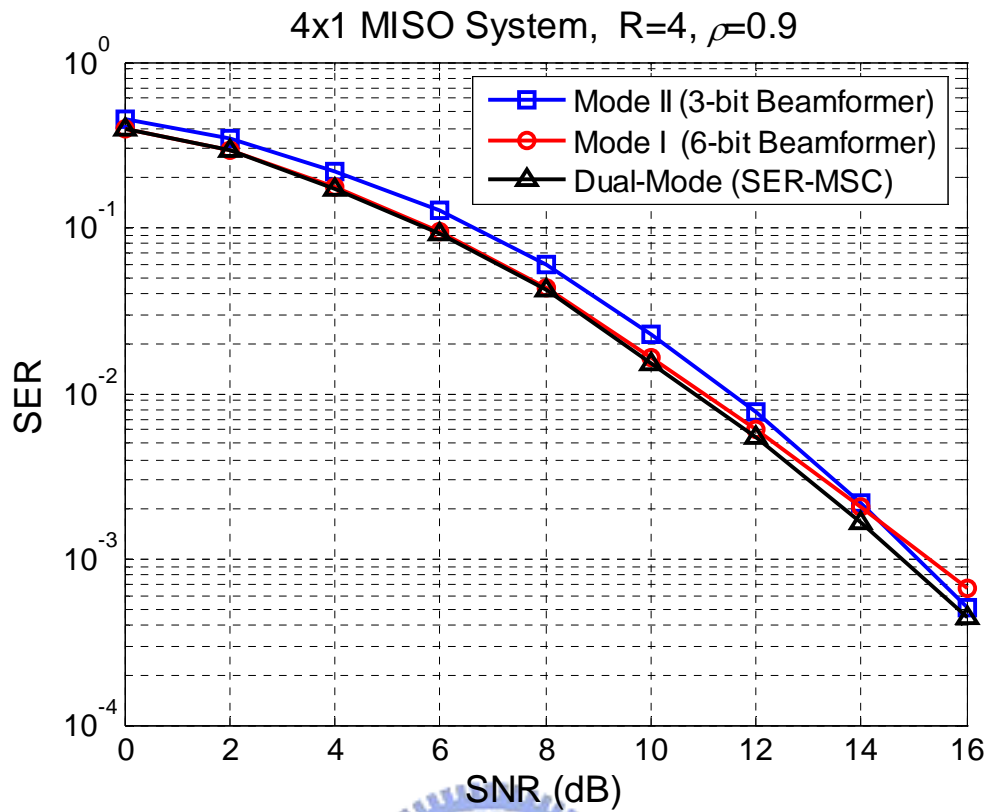**Figure 4.4**: SER performance of the dual-mode 4×1 MISO system with $\rho = 1$

Figure 4.5: SER performance of the dual-mode 4×1 MISO system with $\rho = 0.9$
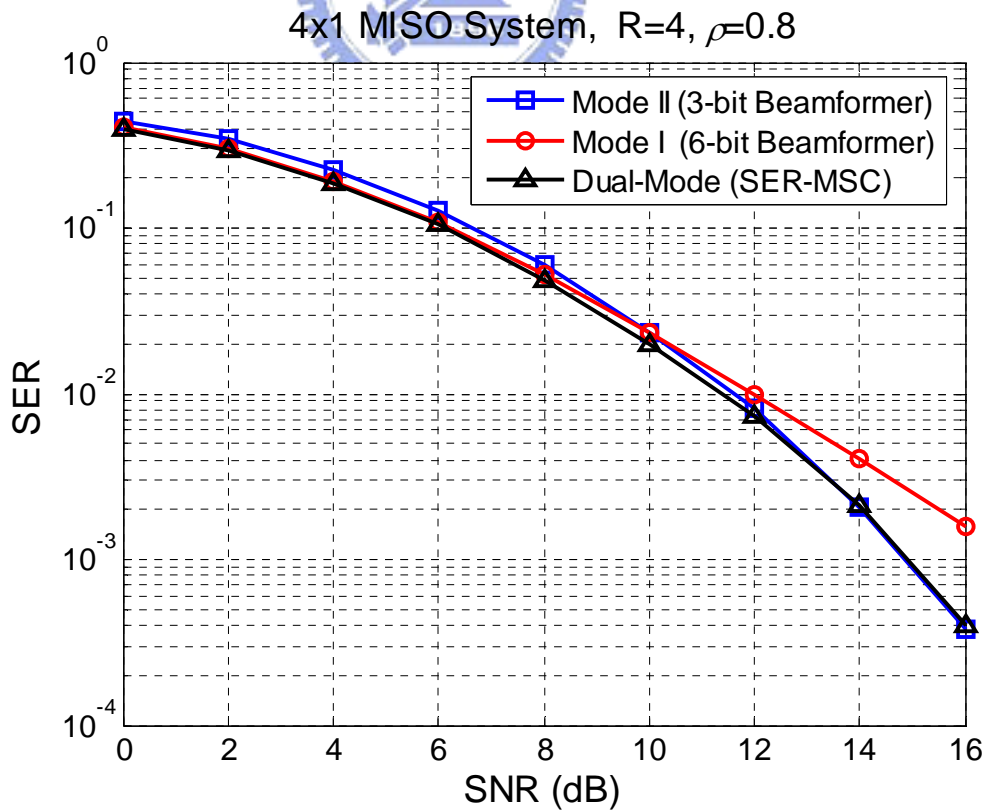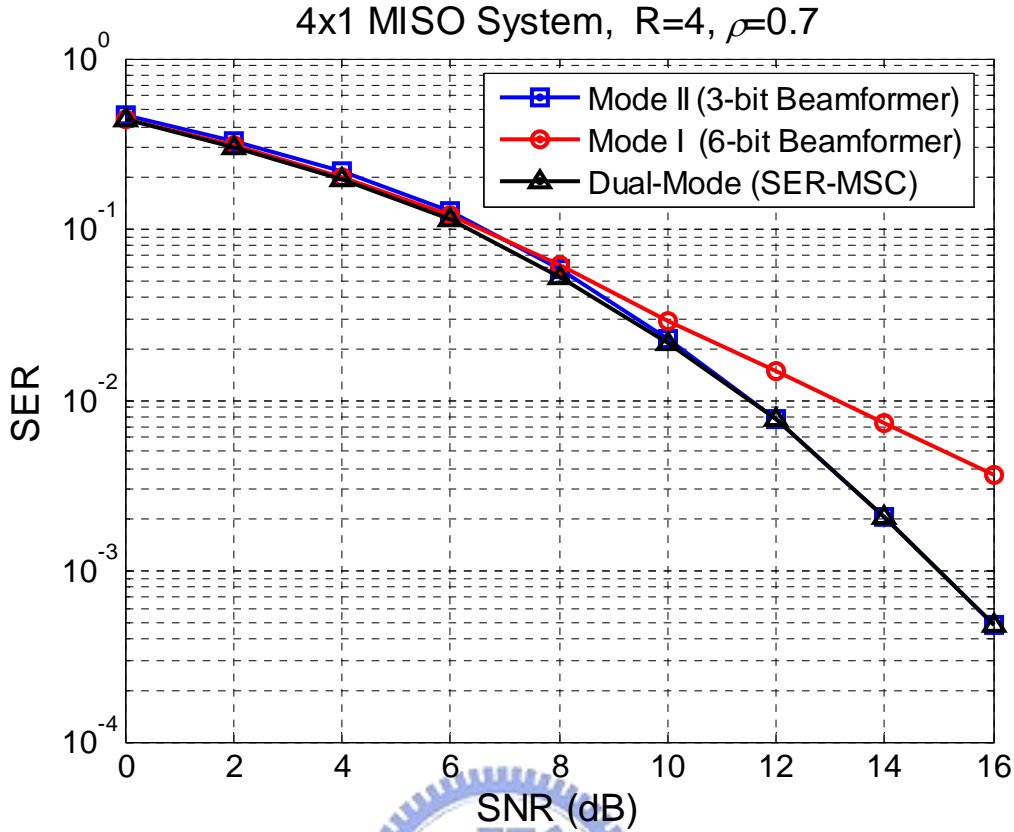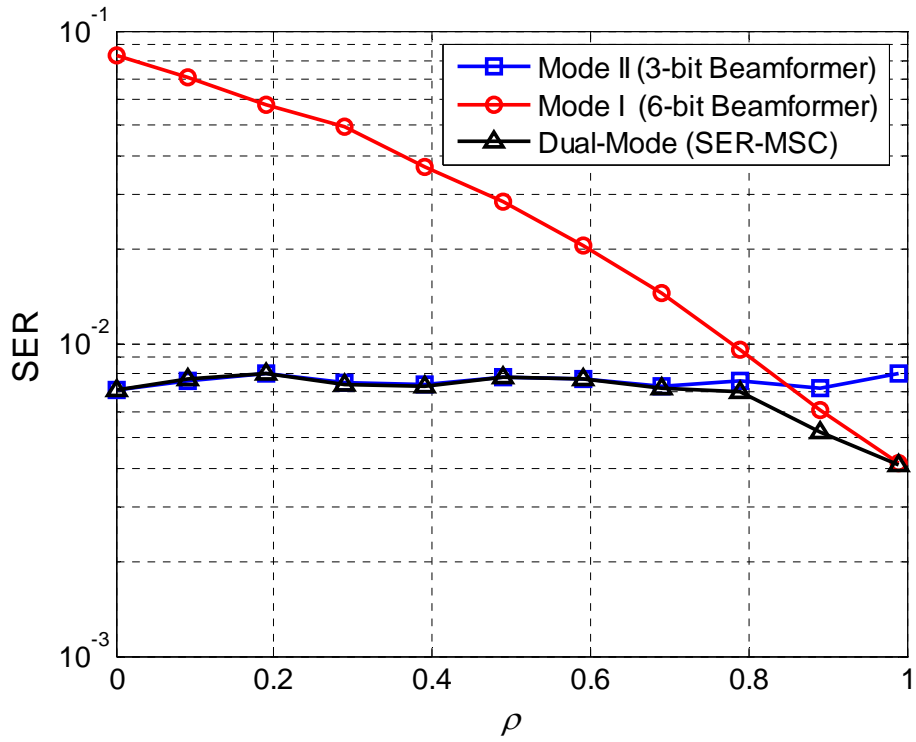

Figure 4.6: SER performance of the dual-mode 4×1 MISO system with $\rho = 0.8$

Figure 4.7: SER performance of the dual-mode 4×1 MISO system with $\rho = 0.7$
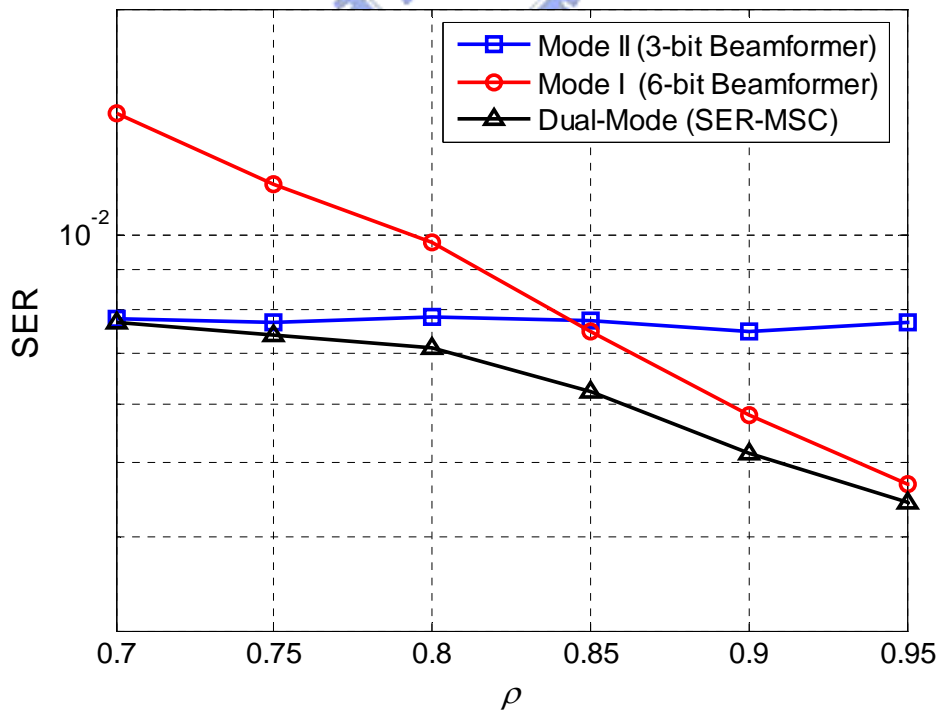
Figure 4.8 shows the SER performance comparison between the single-mode and the dual-mode systems under a fixed SNR=12 dB. **Figure 4.9** shows the SER performance comparison between the single-mode and the dual-mode systems under a fixed SNR=12 dB for $0.7 \leq \rho \leq 0.95$. As we can see, when the channel is subject to high temporal correlation ($\rho \geq 0.85$), Mode I outperforms Mode II, whereas with $\rho \leq 0.85$ the latter yields better performance. The dual-mode system with SER-MSC is more robust than Mode I and Mode II for any ρ. The curve of Mode I crosses the curve of Mode II at about $\rho = 0.85$. In the region $(0.7 \leq \rho \leq 0.95)$, the performance of the dual-mode system is better than that of Mode I and Mode II because the dual-mode system with SER-MSC can select the better mode for current transmission. The dual-mode limited feedback system is more robust in mobile environments.

Figure 4.8: SER performance comparison between the single-mode and the dual-mode

4×1 MISO systems

Figure 4.9: SER performance comparison between the single-mode and the dual-mode

4×1 MISO systems with $0.7 \leq \rho \leq 0.95$

(b) Dual-mode limited feedback MISO-OFDM system

We consider a MISO-OFDM system and **Table 4.2** lists all parameters used in this simulation. This simulation uses 16-QAM modulation and 128 subcarriers in the MISO-OFDM system. Multipath Rayleigh fading channel is used in the simulation. The channel gains of two consecutive OFDM symbol periods follow the first-order Markov channel model (Equation (3.3)), and the relative delays and the average power follow the parameters of the channel model defined in ITU-R M.1225 [37]. The elements of the random perturbation $\Delta\mathbf{h}$ in Equation (3.3) are assumed to be i.i.d. zero-mean complex Gaussian with variance $(1-\rho)$. SNR is defined as the ratio of the average received signal power to the average received noise power after DFT. Perfect channel knowledge known at the receiver and the error-free feedback channel are also assumed in the simulation.

The parameters of the simulation environment of the MISO-OFDM system follow IEEE 802.16-2005 [25] and are stated as follows: The FFT length is 128. The bandwidth is 2.5MHz and the sampling frequency is 2.8 MHz. The sampling time is 357.14 ns and the subcarrier spacing is 21.875 kHz. The ratio of CP time is 1/4. The OFDM symbol time is 57.143 us. Each frame consists of 16 OFDM symbols.

The transmit beamforming codebooks in IEEE 802.16-2005 are applied in the simulation. The average feedback rate is fixed at three bits per tone and per OFDM symbol period. In Mode I, the receiver feeds back six bits to the transmitter **per tone and per two OFDM symbol periods**; in Mode II, the receiver feeds back three bits to the transmitter **per tone and per OFDM symbol period**. The dual-mode limited feedback system selects the better mode between Mode I and Mode II by using SER-MSC. The transmit symbols are precoded tone by tone and we assume that all subcarriers are independent. SER performances of the dual-mode limited feedback MISO-OFDM system with $\rho = 1, 0.9, 0.8, 0.7$ are shown in Figures 4.10-4.13.

Table 4.2: Simulation environment of the dual-mode limited feedback MISO-OFDM system

Parameter	Values					
Channel	Multipath Rayleigh fading channel (First-order Markov channel model)					
Tap (ITU-R M.1225)	1	2	3	4	5	6
Relative delay (ns)	0	310	710	1090	1730	2510
Average power (dB)	0	-1	-9	-10	-15	-20
Bandwidth	2.5 MHz					
FFT length	128					
Sampling frequency	2.8 MHz					
Subcarrier spacing	21.875 kHz					
Useful symbol time	45.714 us					
Ratio of CP time	1/4					
CP time	11.429 us					
Symbol time	57.143 us					
Sampling time	357.14 ns					
Frame length	16 OFDM symbols					
Modulation	16-QAM					
Number of transmit antenna	4					
Number of receive antenna	1					
Fixed average feedback rate	3 bits per OFDM symbol period					
Codebook	Transmit beamforming codebooks in IEEE 802.16-2005					

When $\rho = 1$, **Figure 4.10** illustrates the SER performances of the dual-mode system and the single-mode system. The performance of the dual-mode system is close to that of Mode I and better than that of Mode II. It is observed that the dual-mode system mainly selects Mode I for transmission but not Mode II.

When $\rho = 0.9$, **Figure 4.11** illustrates that the SER performance of the dual-mode system still is better than that of the single-mode system. The curve of Mode II crosses the curve of Mode I at SNR=14 dB. The single-mode system operating in Mode I losses a little diversity gain, but the dual-mode does not. The performance of the dual-mode system is still better than that of the single-mode systems.

When $\rho = 0.8$, **Figure 4.12** shows that the SER performance of Mode I becomes poorer than that of Mode I in **Figure 4.11**. The dual-mode system with SER-MSC is more robust than the single-mode system. At low SNR region, the dual-mode system mainly selects Mode I for transmission. At SNR=10 dB, the dual-mode system can switch between Mode I and Mode II by using SER-MSC, so it has better performance than the single-mode system. At high SNR region, the performance of the dual-mode system is close to that of Mode II. It states that the dual-mode system mainly selects Mode II at high SNR region.

When $\rho = 0.7$, **Figure 4.13** shows that the performance of the dual-mode system is still better than that of the single-mode system. At low SNR region, the dual-mode system mainly selects Mode I; at high SNR region, the dual-mode system mainly selects Mode II. It states that the dual-mode system is more robust than the single-mode system in the time-varying channel.
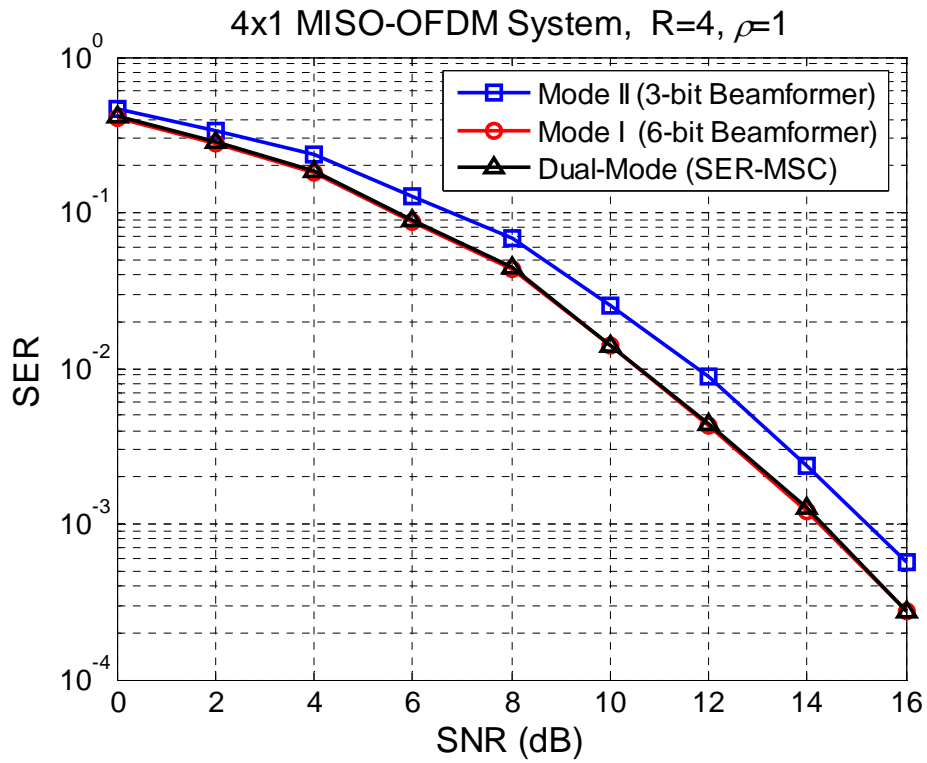
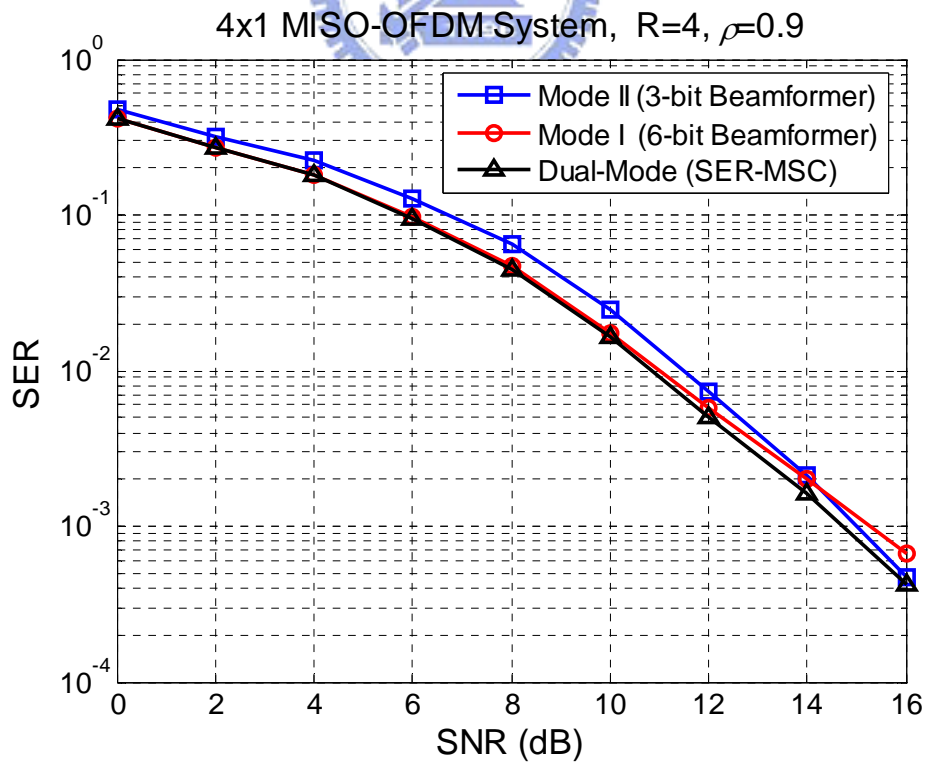**Figure 4.10**: SER performance of the dual-mode 4×1 MISO-OFDM system with
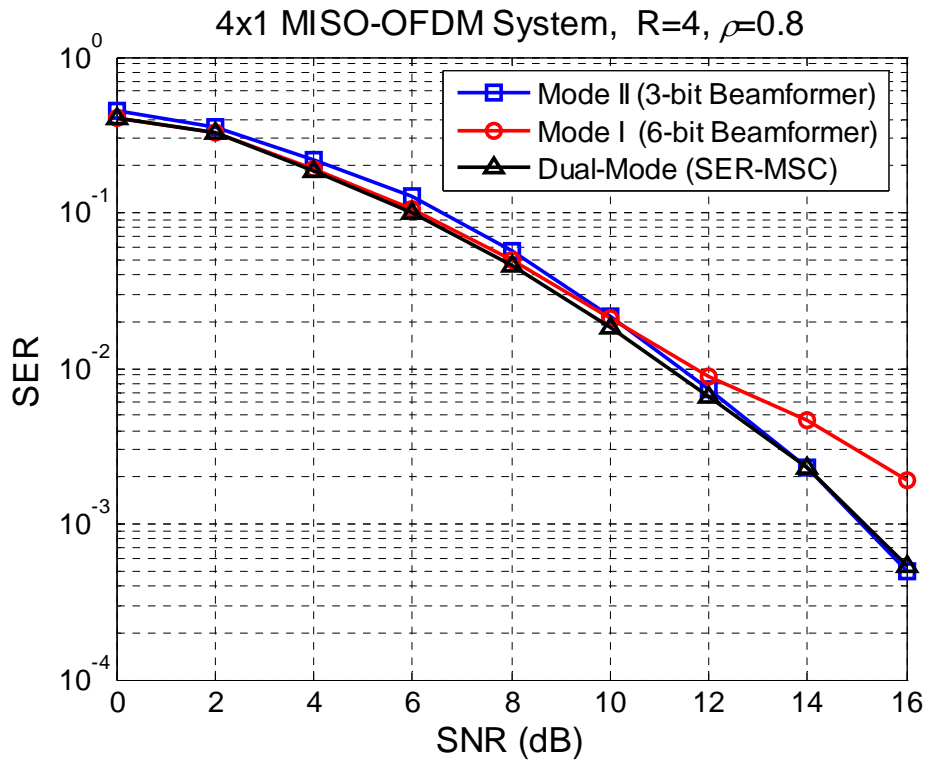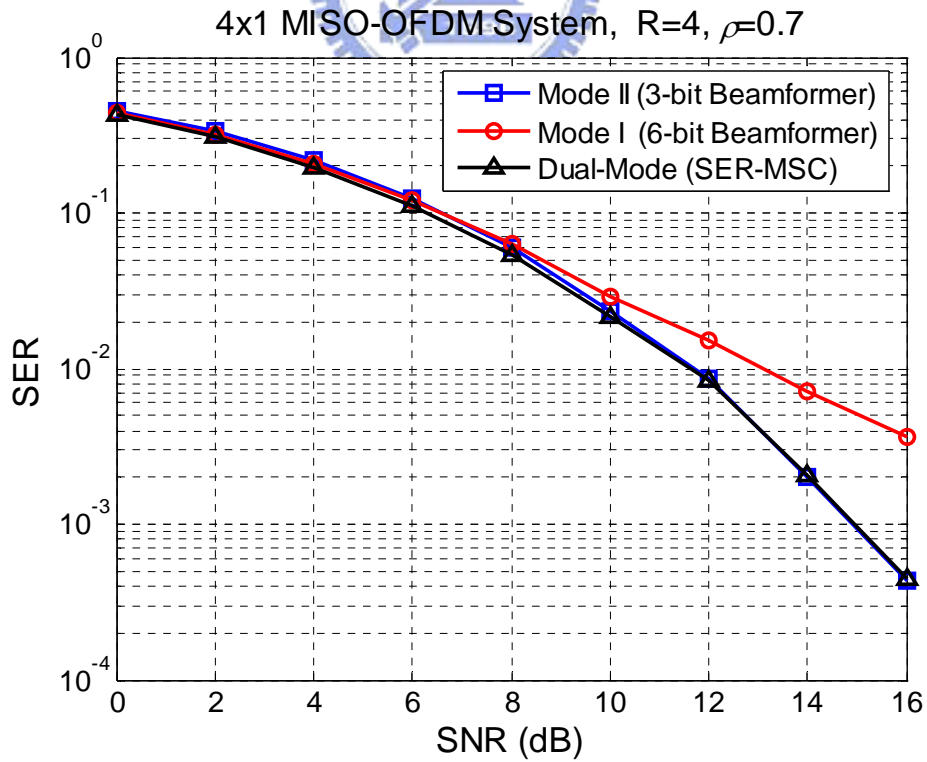
$\rho = 1$

Figure 4.11: SER performance of the dual-mode 4×1 MISO-OFDM system with

$\rho = 0.9$

Figure 4.12: SER performance of the dual-mode 4×1 MISO-OFDM system with
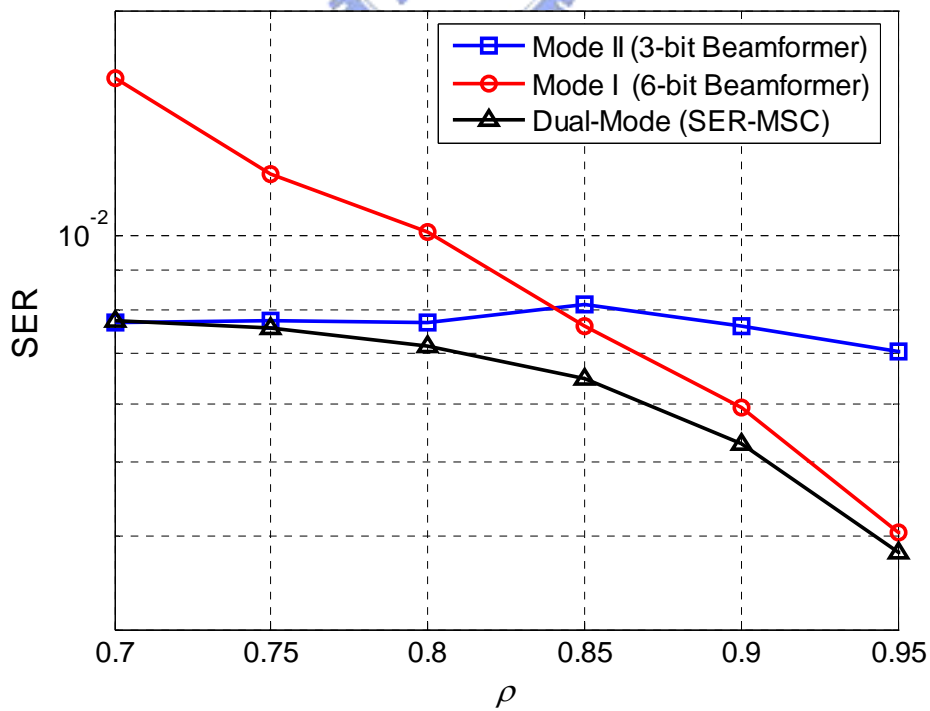
$\rho = 0.8$

Figure 4.13: SER performance of the dual-mode 4×1 MISO-OFDM system with

$\rho = 0.7$

Figure 4.14 shows the SER performance comparison between the single-mode and the dual-mode MISO-OFDM systems under a fixed SNR=12 dB. **Figure 4.15** shows the SER performance comparison between the single-mode and the dual-mode MISO-OFDM systems under a fixed SNR=12 dB for $0.7 \leq \rho \leq 0.95$. As we can see, when the channel is subject to high temporal correlation ($\rho \geq 0.85$), Mode I outperforms Mode II, whereas with $\rho \leq 0.85$ the latter yields better performance. The dual-mode system with SER-MSC is more robust than Mode I and Mode II for any ρ, especially in the region $(0.7 \leq \rho \leq 0.95)$. The dual-mode limited feedback system with SER-MSC can select the better mode for current transmission in mobile environments.

We compare above simulation results with that of MISO systems. It is clearly observed that the results of MISO-OFDM systems are similar to that of MISO systems because the multipath channel response can be reduced into a multiplicative constant on a tone-by-tone basis by discrete Fourier transform (DFT) at the receiver and all subcarriers are independent. The transmitter is precoded with the optimal beamformer tone by tone and the proposed SER-MSC can be equally used in MISO-OFDM systems.
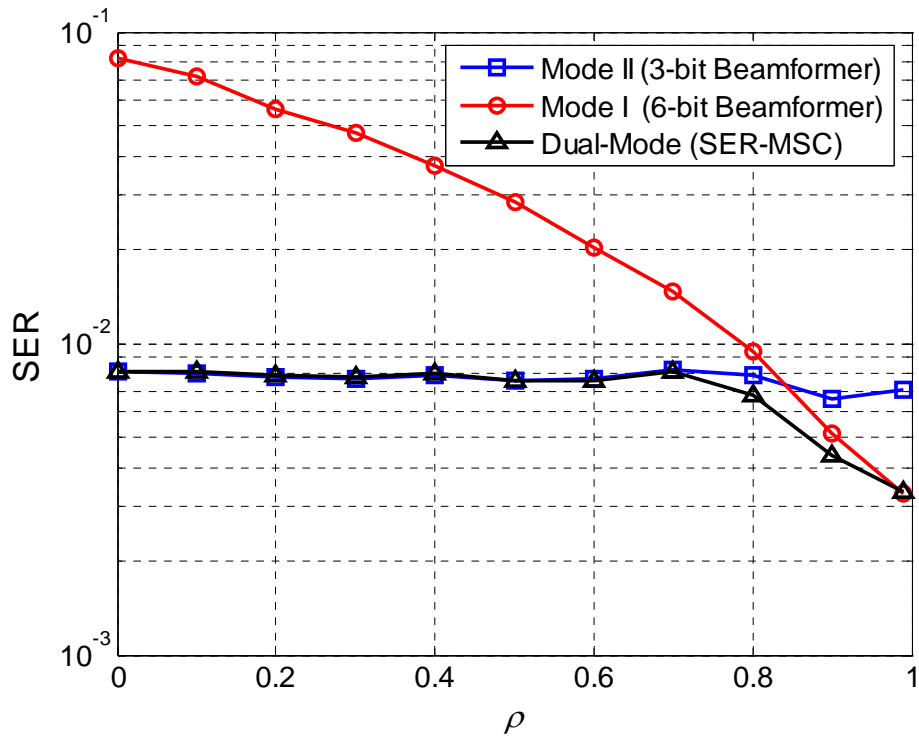
Figure 4.14: SER performance comparison between the single-mode and the dual-mode 4×1 MISO-OFDM systems

Figure 4.15: SER performance comparison between the single-mode and the dual-mode 4×1 MISO-OFDM systems with $0.7 \leq \rho \leq 0.95$

4.5 Summary

We consider the transmit beamforming scheme and MISO channel model in this thesis and use the first-order Markov channel to model the temporal-correlation channels. Under this condition, we propose a dual-mode limited feedback system which has two codebooks with different sizes and an SER based mode selection criterion. From the derivation of SER-MSC, we know that the received signal power gain is a noncentral Chi-square distributed random variable. The simulation results show that the proposed dual-mode limited feedback system is more robust than the single-mode limited feedback system for any temporal-correlation coefficient ρ in mobile environments. Finally, we show the proposed SER-MSC can be equally used in MISO-OFDM systems.

Chapter 5

Conclusion

In this thesis, we introduce two popular approaches for transmission in the MIMO channel: diversity and spatial multiplexing. Precoding is one of the popular schemes to provide diversity gain and additional array gain for improving system performances, but it needs current CSI at the transmitter. Limited feedback systems are proposed to solve the problem. We survey the limited feedback system and explore the precoder selection criteria for selecting the optimal precoder in the limited feedback system. In Chapter 2, we also introduce the codebooks for MIMO precoding schemes in IEEE 802.16-2005, which provides codebooks with different dimensions and sizes depending on the number of transmit antennas and number of data substreams.

In Chapter 3, we introduce the single-mode limited feedback system which has only one codebook for precoding. We consider the MISO channel model and the transmit beamforming scheme because the practical cellular communication system has multiple transmit antennas and one receive antenna in general (e.g., GSM, DCS1800). The first-order Markov channel is used to model the temporal-correlation channels because the model is only characterized by the one-tap temporal-correlation coefficient ρ. The channel can be modeled as a time-invariant channel with a large ρ or a time-varying channel with a small ρ. All codebooks defined in IEEE 802.16-2005 can be divided into two kinds: 3-bit codebooks and 6-bit codebooks. Under a fixed

feedback rate at three bits per frame, Mode I is defined in which the transmitter is precoded with the 6-bit beamformer and the receiver feeds back six bits per two frames; Mode II is defined in which the transmitter is precoded with the 3-bit beamformer and the receiver feeds back three bits per frame. Under this condition, the simulation results show that the single-mode limited feedback systems are not robust in mobile environments. Mode I is suitable to be used in the high temporal-correlation channel and Mode II is suitable to be used in the low temporal-correlation channel.

In Chapter 4, we propose a dual-mode limited feedback system which has two codebooks with different sizes and an SER based mode selection criterion. Based on the average SER over two consecutive frames, the dual-mode limited feedback system can switch between Mode I and Mode II by using SER-MSC. The simulation results show that the dual-mode limited feedback system is more robust and has better performances in mobile environments. We also show that the proposed SER-MSC can be applied to MISO systems and MISO-OFDM systems.

In this thesis, we proposed a dual-mode limited feedback system and derived a SER-MSC used to select the better mode. The dual-mode system can improve system performances based on current CSI in MISO systems or MISO-OFDM systems. It is found that SER-MSC has a high computation cost because of the integration of the PDF of the received power gain. It is not easy to implement this algorithm in hardware. Besides, the assumptions that perfect CSI is available at the receiver, and the feedback channel has zero delay and is error free, may not always hold true. Moreover, it is not practical that each subcarrier uses the individual mode or beamformer in MISO-OFDM systems. Thus, one possible extension of this work is to design a simpler mode selection criterion which is easier to be implemented in hardware. Moreover, the effects of the channel estimation error and nonzero delay, and the subcarrier-grouping based beamforming [23],[38] for OFDM systems are also worth investigating.

Bibliography

[1] I. E. Telatar, "Capacity of multi-antenna Gaussian channels," *Eur. Trans. on Telecommunication*, vol. 10, no. 6, pp.585-595, 1999.

[2] S. M. Alamouti, "A simple transmit diversity technique for wireless communications," *IEEE J. on Selected Areas in Communication*, vol. 16, no. 8, pp. 1451-1458, Oct. 1998.

[3] V. Tarokh, H. Jafarkhani, and A. R. Calderbank, "Space-time block codes from orthogonal designs," *IEEE Trans. on Information Theory*, vol. 45, no. 5, pp. 1456-1467, July 1999.

[4] A. B. Gershman and N. D. Sidiropoulos, *Space-Time Processing for MIMO Communications*, John Wiley, 2005.

[5] H. Sampath, P. Stocica, and A. Paulraj, "Generalized linear precoder and decoder design for MIMO channels using the weighted MMSE criterion," *IEEE Trans. on Communications*, vol.49, no. 12, pp. 2198-2206, May 2002.

[6] Y. Jiang, J. Li and Hager, "Uniform channel decomposition for MIMO communications," *IEEE Trans. on Signal Processing*, vol. 53, no. 11, pp. 4283-4294, Nov. 2005.

[7] M. Vu and A. Paulraj, "Optimal linear precoders for MIMO wireless correlated channels with nonzero mean in space-time coded systems," *IEEE Trans. on Signal Processing*, vol. 54, no. 6, pp. 2318-2332, June 2006.

[8] D. Love and R. W. Heath, "Multimode precoding for MIMO wireless systems," *IEEE Trans. on Signal Processing*, vol. 53, no. 10, pp. 3674-3687, Oct. 2005.

[9] A. Scaglione, P. Stoica, S. Barbarossa, G. B. Giannakis, and H. Sampath, "Optimal designs for space-time linear precoder and decoders," *IEEE Trans. on Signal Processing*, vol. 50, no. 5, pp. 1051-1064, May 2002.

[10] A. Gorokhov, D. Gore, and A. Paulraj, "Diversity versus multiplexing in MIMO system with antenna selection," in *Proc. Allerton Conference on Communication, Control and Compuing,* Oct. 2003.

[11] S. Zhou and G. B. Giannakis, "Optimal transmitter eigen-beamforming and space-time block coding based on channel mean feedback," *IEEE Trans. on Signal Processing*, vol. 50, no. 10, pp. 2599-2613, Oct. 2002.

[12] S. Zhou, Z. Wang, and G.. B. Giannakis, "Quantifying the power loss when transmit beamforming relies on finite-rate feedback," *IEEE Trans. on Wireless Communications*, vol. 3, no. 4, pp. 1948-1957, July 2005.

[13] S. Srinivasa and S. A. Jafar, "The optimality of transmit beamforming: a unified view", *IEEE Trans. on Information Theory*, vol. 53, no. 4, pp. 1558-1564, April 2007.

[14] D. J. Love and R. W. Heath, "Limited feedback precoding for spatial multiplexing systems," *GLOBECOM 2003*, vol. 4, pp. 185-1861, Dec. 2003.

[15] D. J. Love and R. W. Heath, "Limited feedback unitary precoding for orthogonal space-time block codes," *IEEE Trans. on Signal Processing*, vol. 53, no. 1, pp. 64-73, Jan. 2005

[16] D. J. Love and R. W. Heath, "Limited feedback unitary precoding for spatial multiplexing system," *IEEE Trans. on Information Theory*, vol. 51, no. 8, Aug. 2005.

[17] R. W. Heath and A. Paulraj, "Antenna selection for spatial multiplexing systems with linear receivers," *IEEE Communication Letters*, vol. 5, no. 4, pp. 142-144, Apr. 2001.

[18] S. Zhou and B. Li, "BER criterion and codebook construction for finite-rate precoded spatial multiplexing with linear receivers," *IEEE Trans. on Signal Processing*, vol. 54, no. 6, pp. 1653-1665, May 2006.

[19] J. C. Roh and B. D. Rao, "Design and analysis of MIMO spatial multiplexing systems with quantized feedback," *IEEE Trans. on Signal Processing*, vol. 54, no. 8, pp. 2874-2886, Aug. 2006.

[20] E. Lindskog et al., "Closed Loop MIMO Precoding," *IEEE 802.16e-04/293r2*, Nov. 2004.

[21] Q. Li et al., "Improved Feedback for MIMO Precoding," *IEEE C802.16e-04/527r4*, Nov. 2004.

[22] Q. Li et al., "Compact codebooks for transmit beamforming in closed-loop MIMO," *IEEE C802.16e-05/050r6*, Jan. 2005.

[23] C. Zhang et al., "Closed-Loop MIMO Precoding with Limited Feedback," *IEEE C802.16e-04/262r1*, Aug. 2004.

[24] D. J. Love, R. W. Heath, and T. Strohmer, "Grassmannian beamforming for multiple-input multiple-output wireless systems," *IEEE Trans. on Information Theory*, vol. 49, no. 10, pp.2735-2747, Oct. 2003.

[25] IEEE Std 802.16eTM-2005 and IEEE Std 802.16TM-2004/Cor1-2005, "Part 16: Air Interface for Fixed and Mobile Broadband Wireless Access Systems," pp. 587-596, 2005.

[26] A. Narula, M. J. Lopez, M. D. Trott, and G. W. Wornell, "Efficient use of side information in multiple-antenna data transmission over fading channels," *IEEE J. Selected Areas on Communication*, vol. 16, no. 8, pp. 1423-1436, Oct. 1998.

[27] S. Gifford, J. E. Kleider, and S. Chuprun, "OFDM-MIMO communication systems in a Rayleigh fading environment with imperfect channel estimates," *IEEE MILCOM 2003*, vol. 1, pp. 633-637, Oct. 2003.

[28] Z. Liu, X. Ma, G.. B. Giannakis, "Space-time coding and Kalman filtering for time-selective fading channels," *IEEE Trans. on Communication*, vol. 50, no. 2, pp. 183-186, Feb. 2002.

[29] S. H. Ting, K. Sahaguchi, and K. Araki, "A Markov-Kronecker model for analysis of closed-loop MIMO system," *IEEE Communications Letters*, vol. 10, no. 8, Aug. 2006.

[30] G. L. Stuber, *Principles of Mobile Communication*, Kluwer Academic,1997.

[31] E. Visotsky and U. Madhow, "Space-time transmit precoding with imperfect feedback," *IEEE Trans. on Information Theory*, vol. 47, pp. 2632-2639, Sep. 2001.

[32] John G. Proakis, *Digital Communications 4th*, McGrawHill, 2001.

[33] H. Stark and J. W. Woods, *Probability and Random Processes with Applications to Signal Processing 3rd*, Prentice Hall, 2002.

[34] M. Abramowitz and I. A. Stegun, *Handbook of Mathematical Functions with Formulas, Graphs, and Mathematical Tables*, 1967.

[35] N. L. Johnson, S. Kotz, and A. W. Kemp, *Continuous Univariate distributions 2nd*, *Volume 2*, Wiley-Interscience, 1994.

[36] K. K. Mukkavilli, A. Sabharwal, E. Erkip, and B. Aazhang, "On beamforming with finite rate feedback in multiple antenna systems," *IEEE Trans. on Information Theory*, vol. 49, no. 10, pp. 2562-2579, Oct. 2003.

[37] *Recommendation ITU-R M.1225*, "Guidelines for evaluation of radio transmission technologies for IMT-2000," 1997.

[38] N. H. Tran, H. H. Nquyen, and Le-Ngoc Tho, "On subcarrier grouping for OFDM with linear constellation precoding," *2006 IEEE Biennial Symposium on Communications,* pp. 204-208, June 2006.